Marine Geology 377 (2016) 77–94

Contents lists available at ScienceDirect

Marine Geology

journal homepage: www.elsevier.com/locate/margo

Contourite vs gravity-flow deposits of the Pleistocene Faro Drift (Gulf of Cadiz): Sedimentological and mineralogical approaches

Belén Alonso [a,*], Gemma Ercilla [a], David Casas [b], Dorrik A.V. Stow [c], Francisco J. Rodríguez-Tovar [d], Javier Dorador [d], Francisco-Javier Hernández-Molina [e]

[a] Instituto de Ciencias del Mar, Continental Margins Group, CSIC, 08003 Barcelona, Spain
[b] Instituto Geológico y Minero de España, 28003 Madrid, Spain
[c] Institute of Petroleum Engineering, Heriot-Watt University, Edinburgh, Scotland, UK
[d] Departamento de Estratigrafía y Paleontología, Universidad de Granada, 18071 Granada, Spain
[e] Dept. Earth Sciences, Royal Holloway Univ. London, Egham, Surrey TW20 0EX, UK

ARTICLE INFO

Article history:
Received 12 March 2015
Received in revised form 13 November 2015
Accepted 15 December 2015
Available online 14 January 2016

Keywords:
Gulf of Cadiz
Contourites
Turbidites
Debrites
Grain-size
Bulk mineral
Clay mineral

ABSTRACT

Pleistocene succession at Sites U1386 and U1387 (IODP 339) from palaeo-moat and drift domains of the Faro Drift has been examined to characterize the lithofacies and to identify the most useful criteria for distinguishing between contourite and gravity-flow deposits. Three lithofacies, A, B, and C, are defined based on a combination of sedimentological and mineralogical analyses. The dominant lithofacies A corresponds to contourite deposits; lithofacies B and C comprise turbidites and debrites respectively. Three main criteria have been utilized to distinguish between these deposits: (i) the vertical trend of the grain-size and the sedimentary structures. The contourites show complete sequences (C1 to C5 divisions) and truncate sequences (basecut-out divisions, e.g., C3–C2–C1, and C3). The turbidites display mainly Td–Te divisions, although Tc division is also present to a lesser extent. The debrites display deformational and shearing structures; (ii) the modal frequency distribution. The contourite sequences show similar mode grain-size values in different textures suggesting that the steady conditions of supply are maintained over time. In contrast, turbidite and debrite sequences display different modes, primarily conditioned by mixing of components from allochthonous sources and their downslope gravitational transport; (iii) the sediment composition (clay mineral, bulk mineral and sand fraction) and provenance that reflect long- and short-distance transport modes. Most of the terrigenous components of the contourites come from the Guadalquivir drainage basin, whereas for the turbidites and debrites these are sourced from the neighbouring fluvial drainage basins (Guadiana, Tinto-Odiel). The biogenic components in the latter indicate shallow depositional environments prior to seafloor failure. The spatial and temporal distributions of the lithofacies reflect the different (palaeo) environments of the Faro Drift. Debrite and incomplete turbidite sequences characterize the palaeo-moat domain during the Early Pleistocene. Complete contourite sequences (C1 to C5) and basecut-out sequences (C3–C4–C5, and C3) characterize the proximal palaeo-drift domain during the Early and Middle Pleistocene and the complete contourite sequences represent the distal drift domain during the Late Pleistocene.

1. Introduction

The Integrated Ocean Drilling Program (IODP) Expedition 339 (November 2011 to January 2012) drilled five sites in the Gulf of Cadiz and two offshore in western Portugal, and recovered 5.5 km of sediment cores. This expedition provided the opportunity to interpret events (tectonic, climate, sea level changes) occurring around the Gulf of Cadiz in terms of their impacts on regional basin evolution, global ocean circulation, and climate (Hernández-Molina et al., 2016). Five sites, two of them (U1386 and U1387) are analysed in this work, were targeted within the contourite depositional system (CDS) for drilling as a key location for the investigation of Mediterranean Outflow Water (MOW) through the Strait of Gibraltar, and its evolution and environmental implications (Hernández-Molina et al., 2013; Stow et al., 2013). This CDS has developed at very high rates of sediment accumulation over past 5 M.a. as a direct result of MOW, providing an expanded sedimentary record of palaeocirculation linked to past environmental change. Preliminary results indicate a Pleistocene register made up of contourites and some interbedded turbidites (Stow et al., 2013; Hernández-Molina et al., 2014). One of the objectives of that expedition was to identify the sedimentary facies related to the MOW bottom current and the possible interaction between downslope and alongslope processes during the Pliocene and Quaternary (http://iodp.tamu.edu/scienceops/expeditions/mediterranean_outflow.

* Corresponding author.
E-mail address: belen@icm.csic.es (B. Alonso).
gemma@icm.csic.es

http://dx.doi.org/10.1016/j.margeo.2015.12.016
0025-3227/

html). This interplay of processes has been well illustrated on the westernmost part of the Gulf of Cadiz where numerous downslope channels deliver abundant terrigenous material to the continental slope. This region is swept by an active MOW that captures and reworks sediment delivered by downslope processes (Mulder et al., 2006; Marchès et al., 2007, 2010). It is clear that the interplay of downslope and alongslope processes is the rule rather than the exception for deep-water ocean-margin sedimentation, even in isolated drift settings far from a continental source (Faugères and Stow, 1993).

During the last 50 years there have been numerous studies and reviews of criteria for distinguishing between alongslope and downslope and processes (Hollister and Heezen, 1972; Stow, 1979; Stow and Shanmugam, 1980; Johnson and Rasmussen, 1984; Shor et al., 1984; Stanley, 1987, 1993; Locker and Laine, 1992; Faugères and Stow, 1993; McCave and Carter, 1997; Gonthier et al., 2003; Mulder et al., 2006, 2008, 2013). There is no general agreement on diagnostic criteria at a small scale (cores and outcrops) whereas the difference between them is very clear at large scale (depositional systems, on the basis of seismic facies) (Rebesco and Stow., 2001; Llave et al., 2002; Viana, 2001; Hernández-Molina et al., 2006; Roque et al., 2012; Rebesco et al., 2014). At a small scale, several quantitative and qualitative parameters have been used, individually or in combination: grain-size and statistical parameters of their granulometric distribution (e.g., sorting, modal frequency distribution), sedimentary structures, textural vertical trend, mineralogical composition, and magnetic fabric. Various studies (Stow, 1979; Stow et al., 2002; Stow and Faugères, 2008) have argued strongly that a definitive interpretation of contourite facies requires careful combination of small (sediment), medium (seismic) and large-scale (regional) evidence.

Few studies take into account the detailed mineralogical composition and characteristics of contourite and gravity-flow deposits, although this can provide important information about sediment provenance (Stow, 1979; Shor et al., 1984; Stanley, 1987, 1993; Alonso et al., 1999; Martínez-Ruíz et al., 1999). The mineral composition of shelf sediments of the Gulf of Cadiz has been related to the hinterland weathering and to the intensity and direction of the processes responsible for their distribution within the marine environment (Grousset et al., 1988; Gutiérrez-Mas et al., 1995, 1996; Moral Cardona et al., 1997; Machado et al., 2005). In addition, specific clay minerals (e.g., smectite and kaolinite) have been considered of interest for detecting the signal of MOW in the continental slope sediments of the Gulf of Cadiz (Grousset et al., 1988; Vergnaud-Grazzini et al., 1989). In particular, the smectite + kaolinite/illite + chlorite and smectite/illite ratios previously used in this area are seen to be useful for distinguishing particles transported back in the Atlantic Ocean by the MOW and deposited along the Faro Drift (Grousset et al., 1988; Vergnaud-Grazzini et al., 1989). Therefore, the combination of sedimentological and mineralogical criteria can be useful to discriminate between contourite and gravity-flow deposits (turbidites and debrites) in the core material from IODP Expedition 339. For the Gulf of Cadiz slope system, the seismic and regional evidence for contourite sedimentation already exists.

The focus of this study is the Pleistocene sedimentary record from Sites U1386 and U1387, which are located on the Faro Drift on the Algarve margin (Fig. 1). The principal aims are: i) to characterize Pleistocene lithofacies based on sedimentological and mineralogical properties; ii) to identify the main diagnostic features for distinguishing contourite and gravity-flow deposits by examining sedimentological and mineralogical criteria; and iii) to define a model of facies distribution for the depositional architecture of the Pleistocene Faro Drift deposits.

2. Regional settling

2.1. Geological and oceanographic setting

The Gulf of Cadiz, located on the African–Eurasian plate boundary forms a deeply concave indentation between the African and European continental plates (Zitellini et al., 2009; Fig. 1). Its northern margin (Iberian margin) extends off the coast of the SW Iberian Peninsula, from Cape of St Vicente in the west to the Strait of Gibraltar in the east. The Gulf of Cadiz margin can be divided into two sectors, east and west, based on physiographic and sedimentary architecture (Fig. 1A). The eastern sector extending from western Cadiz margin to Huelva margin is progradational. It is marked by the presence of several major tectonic features: the Cadiz and Guadalquivir ridges and the Guadalquivir Bank, and the presence of linear diapiric ridges that are perpendicular to the slope (Maldonado et al., 1999; Nelson et al., 1999; Llave et al., 2002; Garcia et al., 2009, 2015). Fluvial supply is high to the eastern sector. The main fluvial sources are, from east to west: the Barbate, Guadalete, Guadalquivir, Tinto-Odiel, and Guadiana rivers (Fig. 1A). The fluvial discharges of these rivers are very irregular, with significant seasonal and interannual variability (Borrego et al., 1995). The Guadalquivir River has the highest mean water discharge (164 $m^3\ s^{-1}$) into the Gulf of Cadiz (Palanques et al., 1995) and the Guadiana River has the second highest. The mean annual discharges show considerable variability (80–140 $m^3\ s^{-1}$) reaching peak discharge of 3000 $m^3\ s^{-1}$ in the winter. The Tinto-Odiel and Guadalate rivers have low mean annual discharges (1 and 10 $m^3\ s^{-1}$).

The western sector of the Gulf of Cadiz, the Algarve margin, is relatively more narrow and steep margin. This margin is scoured by erosional features (including canyons and linear channels) and is interrupted by a marginal plateau between 600 and 800 m water depth (Mougenot, 1988; Marchès et al., 2007, 2010; Brackenridge et al., 2013). Fluvial supply is low to moderate with small fluvio-estuarine systems. The main sources of sediments to the margin are from cliffs erosion and river input with ephemeral discharges (e.g., Quarteira and Portimao rivers; Roque et al., 2010; Rosa et al., 2013).

The surficial shelf sediments of the Gulf of Cadiz are characterized as follows (Fig. 1A): i) a continuous belt of sandy deposits, in particular bioclastic quartzose sands, on the inner shelf of the easternmost sector (Cape of Trafalgar—Cadiz); this trend is interrupted in the proximity of the most important river mouths (Guadiana and Guadalquivir), in front of which more mud-rich patches occur; ii) mud on the mid-outer shelf, locally interrupted by sandy sediments off the Guadiana River; iii) clayey sand, sandy and silty clay, and large patches of relict sand and gravel on the shelf break (Gutiérrez-Mas et al., 1996; Fernández-Salas et al., 1999; López-Galindo et al., 1999; González et al., 2004; Lobo et al., 2014); and iv) reworked relict sand with a high content of ultra-stable heavy minerals and bioclastic particles over the Barbate continental shelf, SE of the Bay of Cadiz. Toward the Strait of Gibraltar, the surficial shelf sediments show an increase in gravel and local rock outcrops of Betic and flysch units from the Campo de Gibraltar complex (López-Galindo et al., 1999; Nelson et al., 1999).

On the middle continental slope of the Gulf of Cadiz, an extensive contourite depositional system (CDS) was generated during the Pliocene and Quaternary (Fig. 1B, C). This CDS extends in a generally E-W direction along the middle continental slope (e.g., Gonthier et al., 1984; Nelson et al., 1999; Stow et al., 2002; Alves et al., 2003; Habgood et al., 2003; Hernández-Molina et al., 2003, 2006, 2008; Mulder et al., 2003; Hanquiez et al., 2007; Llave et al., 2007a,b; Marchès et al., 2007; Roque et al., 2012; Brackenridge et al., 2013). One of the main depositional features of this CDS is the Faro Drift (Faugères et al., 1984; Gonthier et al., 1984; Llave et al., 2006), which is located at ~500–1100 m water depth (Fig. 1B). The Faro Drift has a total length of 100 km, a maximum width of 20 km, a relief of 200 m and a maximum thickness of ~700 m and comprises both erosive (moat) and depositional features (drift) (Fig. 1C). It is limited by the Faro and Portimao canyons to the west and a sinuous contouritic moat (Alvarez Cabral) to the north, and merges southward above the adjacent sheeted drift platform region, where it is deeply incised by the Diego Cao Channel (Stow et al., 2002; Fig. 1B).

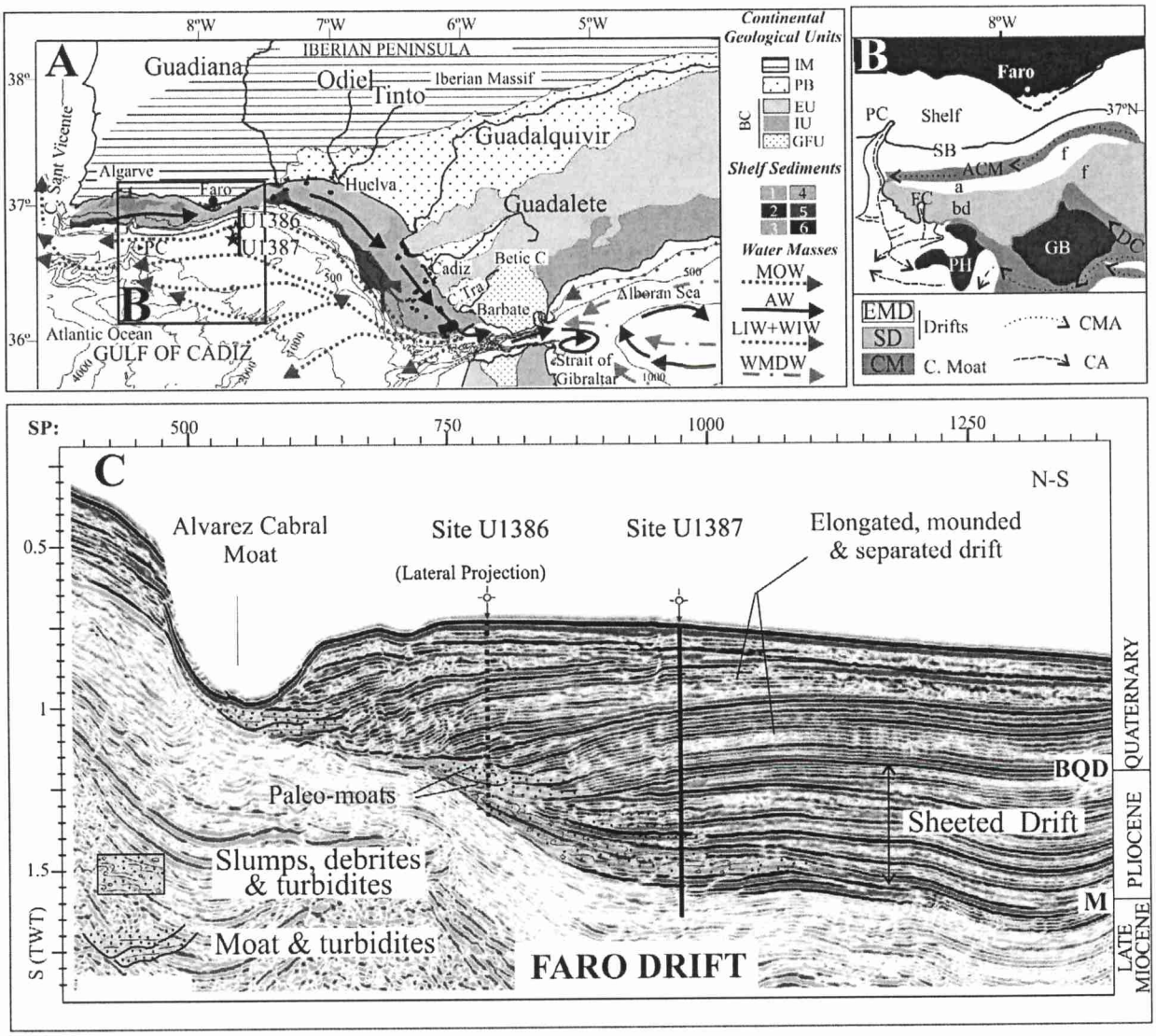

Fig. 1. General setting of the study area in the Gulf of Cadiz: A) geological map showing the river basin drainage with the main continental geological units (modified from Gutiérrez-Mas et al., 2003), shelf sediments (modified from Lobo et al., 2014) with regional bathymetry and the general oceanographic circulation pattern (modified from Hernández-Molina et al., 2006), and the location of the study sites; B) morphosedimentary features of the Faro (f), Albuferia (a) and Bartolomeu Dias (bd) drifts; and C) stratigraphic section displaying the major sedimentary deposits from the Pliocene and Quaternary of the Faro Drift (modified from Hernández-Molina et al., 2014). Legend: IM, Iberian Massif; PB, Postorogenic Basins; BC, Betic Cordillera; EU, External Units; IU, Internal Units; GFU, Gibraltar Flysch Units. 1, coastal and inner shelf sands; 2, proximal prodeltaic muds; 3, middle shelf sands; 4, middle shelf muds; 5, outer shelf sands; and 6, rocky outcrops. MOW, Mediterranean Outflow Water; AW, Atlantic Superficial Water; WIW + LIW, Western Intermediate Water, and Levantine Intermediate Water; WMDW, Western Mediterranean Deep Water; C, Cape of; C. Tra. cape of Trafalgar; EMD, elongated mounded drift; SD, sheeted drift; CMA, contourite moat axis; CM, contourite moat; CA, canyon axis; SB, shelf break; GB, Guadalquivir Bank; PH, Portimao High; PC, Portimao Canyon; FC, Faro Canyon; DC, Diego Channel; ACM, Álvares Cabral Moat. The thick line in A refers to the seismic profile in Fig. 1C. Contours in metres.

The hinterland domain of the Gulf of Cadiz comprises several geological formations, including the Betic and Rif Cordillera, the Iberian Massif and the Guadalquivir Basin (Fig. 1A). The Betic and Rif Cordillera contain (Galindo-Zaldívar et al., 1997; Maldonado et al., 1999): i) the metamorphic complexes of the Internal Zones, ii) sedimentary units of the External Zones, and iii) the Flysch domain consisting of thick, mainly turbidite sequences (Didon et al., 1973). The Iberian Massif is formed of metasediments and greywackes which are drained mainly by the Guadiana River and to a lesser extent by the Guadalquivir River (Oliveira et al., 1979). Some metasediments (phyllite and quartzite and volcanic rocks) are found in the south Portuguese zone, although the majority of this region is covered by turbidite sequences (Galindo-Zaldívar et al., 1997). Between the Iberian Massif and the External Zones is situated the Neogene Guadalquivir Basin, which is filled with siliciclastic and carbonate sediments (clays, sands and conglomerates) with olistostromes emplaced from the External Zones on its southern edge (Perconig and Martínez-Díaz, 1977; Roldán-García and García-Cortés, 1988; Alves et al., 2003).

The present-day water masses in the Gulf of Cadiz are driven by the density contrast between the water masses of Atlantic (cold, normal salinity, less dense) and Mediterranean (warm, higher salinity, more dense; Levantine Intermediate Water, Western Intermediate Water and Western Mediterranean Deep Water) origin that flow through the Strait of Gibraltar (Mélières, 1974; Baringer and Price, 1997; Ercilla et al., 2015). This water exchange is characterized by the eastward upper layer of Atlantic Water into the Mediterranean Sea and a westward bottom layer of the MOW. It is the bottom current generated by the MOW that is responsible for forming the contourite deposits

of the Faro Drift (Gonthier et al., 1984). Surface Atlantic Water flows (0–500 m water depth) eastward over the Gulf of Cadiz continental shelf (Lobo et al., 2001) into the Mediterranean and is responsible for distributing the fine sediments supplied by the main rivers to the continental shelf (Grousset et al., 1988; Gutiérrez-Mas et al., 1995). A SE-directed littoral drift, resulting from the predominant W and SW storms, is the dominant factor in moving sediment along the shoreline and across the shelf (Gutiérrez-Mas et al., 1996, 2003).

2.2. Faro Drift: stratigraphy and lithological units

Seismic-stratigraphic studies reveal that the Faro Drift has been constructed from Pliocene to the present day in different phases that show different stacking patterns (Stow et al., 2013; Hernández-Molina et al., 2014, 2016). The weakly reflective Miocene unit is of pre-contourite construction (Fig. 1C). The Pliocene deposits that overlie the Messinian discontinuity (M seismic reflector in Fig. 1C) have built upwards as a sheeted drift. The Quaternary deposits are separated from the Pliocene by the Base Quaternary Discontinuity (BQD in Fig. 1C) and appear as mounded, separated drift deposits with clear oblique alongslope progradation. A general lateral migration of the palaeo-moats found within the Pliocene and Quaternary indicates a steady lateral migration of the drift-moat system and progressively greater confinement of the moat against the slope (Stow et al., 2002; Roque et al., 2012; Hernández-Molina et al., 2014; Fig. 1C). Stratigraphic correlation and specific age constraints of the Sites U1386 and U1387 were established by IODP Expedition 339 using several approaches (lithostratigraphy, biostratigraphy, palaeomagnetic data, geochemical analysis, and borehole logs) (Expedition 339 Scientists, 2012). Age data were used to determine the ages of key seismic horizons (including several hiatuses and stratigraphic boundaries) and the sediment accumulation rates (Fig. 2).

At Site U1386 two lithological units (I and II) were identified (Fig. 2A): i) Unit I (~0–418 m below sea floor [mbsf]), Holocene–Pleistocene in age, is subdivided into three subunits (IA, IB, IC) and is dominated by classical contourite deposition with thin turbidite

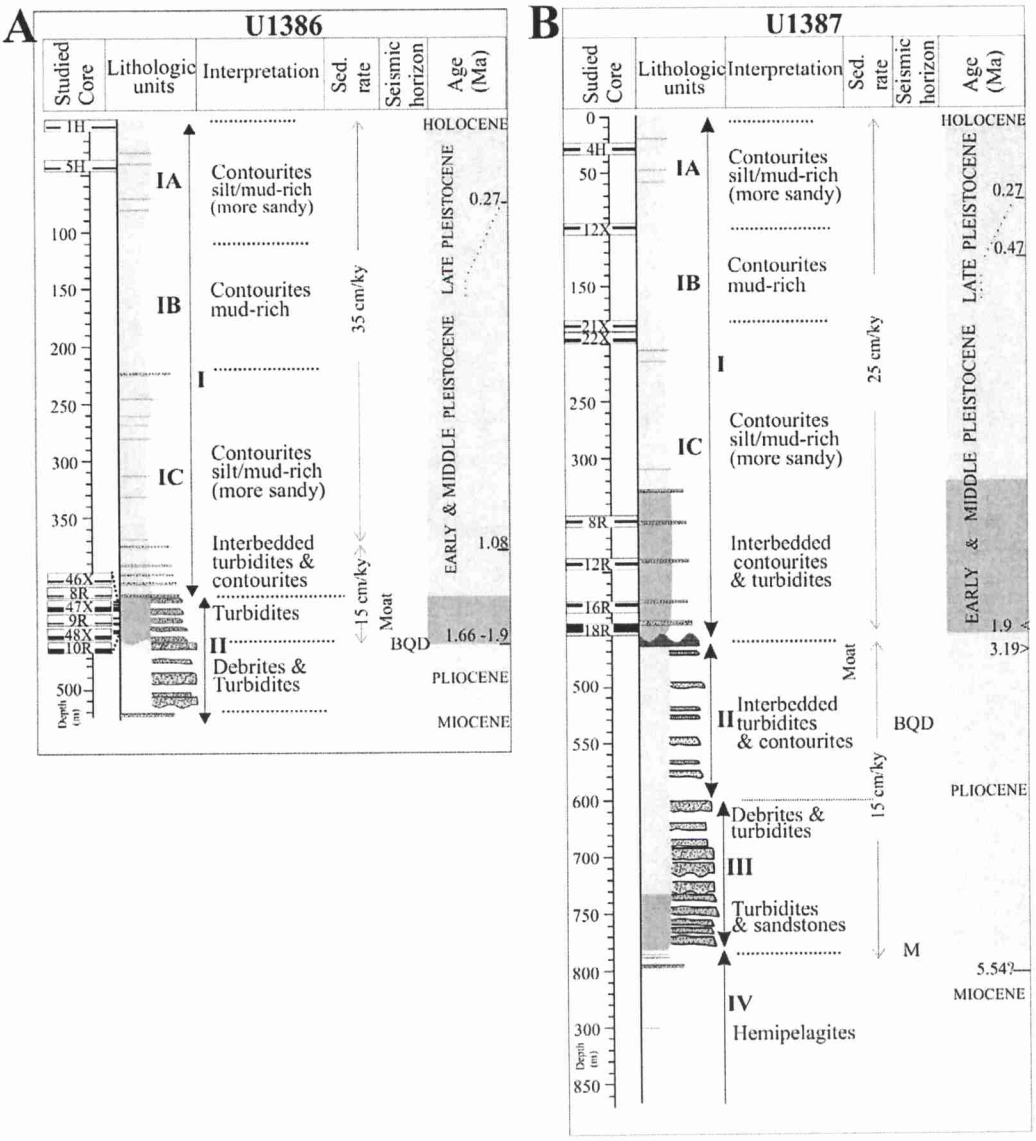

Fig. 2. Plio-Quaternary lithostratigraphic units from Sites U1386 (A) and U1387 (B) of the Faro Drift (based on Expedition 339 Scientists, 2012). The rectangle refers to the studied core and the thick black line corresponds to the studied core section. For more details of the studied holes and core sections, see Section 3. Legend: BQD, Lower Quaternary seismic reflector; M, Messinian seismic reflector.

intercalations in the lowermost 30 m of subunit IC; ii) Unit II (~418–530 mbsf), Miocene–Pleistocene in age, is characterized by turbidites and debrites interbedded with contouritic and hemipelagic nannofossil muds. The Pleistocene units (Unit I and upper part of Unit II) were deposited at moderate sediment accumulation rate (15–35 cm/ky). At Site U1387 four lithological units (I–IV) were identified (Fig. 2B): i) Unit I (~0–450 mbslf), Holocene–Pleistocene in age, is subdivided into three subunits (IA, IB, and IC). It is dominated by classic contourite deposition with thin turbidite intercalations which are predominantly found in the lowermost section; ii) Unit II (~450–595 mbsf), Pliocene in age, is characterized by the same lithologies as in lower part of Unit IC; iii) Unit III (~600–746 mbsf) is mainly Early Pliocene in age, but may start in the latest Miocene. This unit comprises poorly sorted turbidites, chaotic debrites and slumps; and iv) Unit IV, Late Miocene in age, is dominated by hemipelagic sediments, mainly nannofossil muds and muddy oozes. The two studied sites (U1386 and U1387) have been projected on the seismic profile showed in Fig. 1C (Expedition 339 Scientists, 2012) providing information about the lithostratigraphy of palaeo-moat and drift domains (Fig. 1C). The lithostratigraphy of the palaeo-moat domain is recorded in the upper part of Unit II at Site U1386 and that of the drift domain is recorded in the subunit IA of Site U1386 and in the subunits IC, IB and IA of U1387 (Figs. 1C and 2).

3. Material and methods

3.1. Location

Two sites, U1386 and U1387, have been studied on the Faro Drift (Fig. 1A, C). Site U1386 (drilled over 526 mbsf) is located at 561 m water depth (36°49.685′N; 7°45.321′W) close to the Alvarez Cabral moat. Site U1387 (drilled over 820 mbsf) is located at ~559 m water depth (36°48.321′N; 7°43.1321′W), south-southeast of the Portuguese city of Faro, about 4 km from Site U1386, in the eastern part of the Faro Drift (Stow et al., 2013). We examined the following Pleistocene lithological units and subunits: IA (Holes U1386B and U1387A), IB (Hole U1387A), IC (Hole U1387C) and uppermost part of Unit II (Holes U1386B and U1386C). In particular, a total of 149 samples were selected from four holes basis onboard description, lithostratigraphy, and photos (U1386B, U1386C, U1387A and U1387C). The sections and age of sediments studied for each hole are as follows (Fig. 2):

i). Hole U1386B: sections 1H2 and 5H4 (subunit IA, Late Pleistocene); sections 46X5, 47X1, 47X2, 47XCC, 48X2, 48X3 (upper part of Unit II—Early Pleistocene).
ii). Hole U1386C: 8R2, 9R2, 10R3, 10R6 and 10RCC (upper part of Unit II—Early Pleistocene).
iii). Hole U1387A: section 4H5 (subunit IA–Late Pleistocene), section 12X4 (subunit IB, Middle Pleistocene), sections 21X4 and 22X6 (subunit IC—Middle Pleistocene).
iv). Hole U1387C: sections 8R5, 12R3, 16R3, 16R4, 18R2, 18R4, 18R5 and 18R7 (subunit IC—Early Pleistocene).

3.2. Methods

The grain-size was obtained using a Coulter LS 100 laser particle size analyser (CLS) that determines particle grain-sizes between 0.4 and 900 mm as volume percentages based on diffraction laws (McCave et al., 1986). Prior to measurement, we treated the ~10 g samples with hydrogen peroxide to remove organic matter. A cumulative curve and frequency histogram were plotted for the grain size distribution for each sample. Textural statistical parameters were established using the GRADISTAT software (Blott and Pye, 2001). These parameters were calculated using moments (geometric) methods on sample populations. The degree of sorting (standard deviation) was established using the Folk and Ward (1957) classification.

The carbonate content and sand fraction were analysed in terms of sediment composition. Total carbonate content was determined using a Bernard calcimeter (Alonso et al., 1996). For the sand fraction composition (320 grains per sample were counted) was examined using a binocular microscope. Terrigenous components were classified as quartz, mica, rock fragments, pyritized material and burrows, and glauconite. Biogenic components were classified as planktonic foraminifera (entire and fragments), benthic foraminifera, ostracods, bivalves, and gastropods. Quartz grains were examined by SEM.

Ichnological analysis was based on an integrative method using digitally treated high-resolution images from selected core intervals. Sections U1386B 46X5, 47X1, 47X2 and 48X2 and sections U1386C 10R3, 4H5 and 16R3 covering the main deposit types (contourite and gravity-flow deposits) as defined onboard during Leg 339 were selected for this purpose (Stow et al., 2013). The digital image treatment used here was recently developed and applied in cores from IODP Expedition 339 (Dorador and Rodríguez-Tovar, 2016; Rodríguez-Tovar et al., 2015a,b; Takashimizu et al., 2016). This integrative method improves ichnological investigation in soft sediment, enabling definition of ichnotaxa, differentiation between biogenic structures and host sediments (Dorador et al., 2014a), evaluation of the percentage of bioturbated structures (estimation of the amount of trace fossils produced by a particular ichnotaxon, by a whole ichnocoenosis or for a complete ichnofabric) (Dorador et al., 2014b), and characterization of ichnological features such as cross-cutting relationships and tiering patterns (Dorador and Rodríguez-Tovar, 2014; Rodríguez-Tovar and Dorador, 2015). Colour photos were taken from all the studied cores to complement the digital image treatment and the visual core descriptions undertaken on board Leg 339 in order to define sedimentary structures, type of sequence and thickness.

Bulk and clay mineral composition were analysed by X-ray diffraction (XRD) in order to identify mineral composition and help infer provenance. This mineralogical analysis was performed with a Bruker-AXS D8-A25 diffractometer equipped with a Cu tube (Lambda = 1.5405 Å) and an ultra-fast (Lynxeye) detector. For bulk mineralogy, a representative and homogenized part of each sample was used prior to the bulk mineralogic analysis; samples of about 3 g of bulk sediment were air-dried, ground and homogenized with an agate mortar. The relative abundance of the dominant clay fraction components including quartz, calcite, dolomite, and clay minerals was estimated using the intensity of their main diffraction peaks. For clay mineralogy, scans from 2° to 40° (2Θ) were performed on oriented clay fraction samples (untreated, glycolated, and heated to 550 °C). The samples were disaggregated obtaining a suspension of an amount of 500–1000 mg of sample in distilled water (10–15 ml) in a test tube, and softly shaken. After 60 s of natural sedimentation, we get the superior fraction with a pipette and put this on a glass slide that fits on the diffractometer sample holder. The first analysis is made without any treatment. The ethylene glycol solvation treatment involves placing the samples in a solvate vapor medium for not less than 48 h. The final treatment consists of placing the glass slides in a furnace at 550° for two hours. Diffraction profiles were visually interpreted with the help of a computerized search. The relative clay mineral proportion was estimated following the method of Chung (1974), and the peak heights for each mineral were considered as previously reported for sediments from southern Iberia (Algarve, Cadiz and Alboran; Grousset et al., 1988; Vergnaud-Grazzini et al., 1989; Heimhofer et al., 2008). The peak heights used were 10-Å (001) for illite, 7.17-Å (001) for kaolinite, 17-Å for smectite and 14-Å (001) for chlorite. Note that the main reason for the estimated semi-quantitative analysis is to show changes or gradients in mineral abundance rather than absolute values. In addition to clay mineral percentages, we systematically calculated the smectite/illite (S/I) ratio and smectite + kaolinite/illite + chlorite (S + K/I + C) ratio corresponding to the ratio of their peak heights.

We use the term lithofacies as the "sum total of lithological characteristics of a sedimentary rock" such as lithology, grain-size, mineralogy, petrology, physical and biogenic sedimentary structures, and stratification that bear a direct relationship to the depositional processes that produced them (Weller, 1958; Maldonado and Stanley, 1976; Jenner et al., 2007).

4. Results

4.1. Lithofacies

Three main lithofacies A, B and C, were defined based on a cluster of classic and fundamental qualitative and quantitative sedimentological, and mineralogical attributes that include assemblages of the following elements (Alonso et al., 2014): i) grain-size distribution; ii) structures and ichnofacies iii) carbonate content and sand fraction composition; and iv) bulk and clay mineralogical composition (Table 1).

4.1.1. Grain-size distribution

Lithofacies A consists of muddy and fine sandy sediments which are represented by three textures: (1) silty-clay (mean 4–6.2 μm), (2) clayey-silt (mean 9–17 μm), (3) clayey–sandy silt and silt (mean 19–54 μm), and sand (mean 72 μm, in only one sample). It has mainly bi-modal and tri-modal frequency distributions (Fig. 3). The modal frequency distributions of each textures are as follows (Fig. 3): (1) silty-clay: 4–11–26 μm, 4–10–66 μm (e.g., U1387A 21X4) and 4–9–24 μm, 10–26 μm (e.g. U1386A 4H5); (2) clayey silt: 61–26–4 μm, 55–11–4 μm (e.g., U1387A 21X4), and 66–10–4 μm and 55–10 μm (e.g., U1386A 4H5); (3) clayey–sandy silt and silt: 70–9-4 μm, 70–11–4 μm (e.g., U1387A 21X4), and 73–10–4 μm, and 73–10 μm (e.g., U1386A 4H5). This lithofacies is poorly sorted (>3 μm). The vertical succession of grain-size displays a progressive increase and then decrease of grain-size, referred to as a bi-gradational pattern (coarsening-up and fining-up). The complete vertical succession begins at the base with fine-grained mud (texture 1), passing upwards mottled to silt (texture 2), then sandy silt or very fine sand (texture 3), and then repeats these textures again but in the opposite order, passing to mottled silt (texture 2) and then homogeneous fine-grained mud (texture 1). The complete vertical succession of textures 1–2–3–2–1 is only observed in three sections (U1386B 1H2 and 5H4; U1387 4H5). Mostly, we observe partial bi-gradational succession of textures (1–3–2–1 or 1–3–1 (Fig. 4). The thicknesses of these successions are generally between 10 and 60 cm, with the exception of one thicker sequence (up to 90 cm) (section U1387C 16R3). Through a single vertical succession, the modal frequency distribution shows similar modal grain-size and only the relative abundance of the modes varies (Fig. 3).

Lithofacies B comprises fine-grained sediments and shows three textures: (1) clayey-silt, (2) silt and sandy-silt (mean 3–10 and 8–30 μm, respectively), and (3) silty-sand (mean 52–115 μm, reaching 142 μm only in two samples). This lithofacies has uni- bi- and tri-modal frequency distributions with variable mode values throughout the lithofacies. The modal frequency distribution of the different textures is as follows (Fig. 3): (1) clayey-silt: 7–19–50 μm (U1386B 46X5), 10–46 μm (U1386B 47X2), (2) silt and sandy silt: 154–20–7 μm (U1386B 46X5), 154–20–7 μm (U1386B 46X5), 60–16 μm (U1386B 47X2), and (3) silty-sand: 169–38 μm, and 245–127–30 μm. This lithofacies is poorly sorted (>3 μm). The vertical succession of grain-size shows normal grading from silt to mud with a sharp contact at the base. The thicknesses of individual succession vary from 1 cm to at least 95 cm (Fig. 4).

Lithofacies C consists of finer-grained sediments represented by two textures: (1) clayey-silt, and (2) clayey–sandy silt and silt (mean 4–9 μm, 9–16 μm, and 7–10 μm, respectively). It has bi- and tri-modal patterns of modal frequency distribution similar to that defined for lithofacies B. The modal frequency distribution of each texture is as follows (Fig. 3): (1) clayey-silt: 4–11–26–55 μm (U1386C 10R6), and (2) clayey–sandy silt and silt: 11–47 μm, 20–66 μm (U1385C 10R3) and silt: 50–11 μm, and 73–6–21 μm. This lithofacies is poorly sorted sediments (>3 μm). There are no distinct vertical trends of grain-size displaying matrix-supported mud-clast beds (Fig. 4). The thickness of individual beds is from 50 to 100 cm.

4.1.2. Structures and ichnofacies

Lithofacies A is moderately to intensively bioturbated. Two ichnofabric types are recognised (numbers 1 and 2 in Fig. 5): 1) a well-developed mottled silt background, mainly consisting on biodeformational structures overprinted by scarce trace fossils (*Planolites, Thalassinoides-like and Ophiomorpha-like*) especially in mottled silts and silts; 2) homogeneous muds with some trace fossils infilled by relatively coarser sediments (silts) from the overlying lithofacies (yellow stars in Fig. 5). Lithofacies B displays two ichnofabric types (numbers 3 and 4 in Fig. 5): 3) a well-developed

Table 1
Summary of the main characteristics of muddy contourite (LA), turbidite (LB) and debrite (LC) lithofacies of Pleistocene Faro Drift deposits. Legend: Carb. Cont., carbonate content; Sand Frac., sand fraction composition; XRD., X-ray diffraction; and S. Seq., sedimentary sequence.

		Muddy contourites (LA)	Turbidites (LB)	Debrites (LC)
Texture	✓	Fine-grained sediments (4–54 and 72 μm)	Fine-grained sediments (3–52, and 52–142 μm)	Fine-grained sediments (4–16 μm)
	✓	Silty muds alternate with fine-grained sands and silts	Clayey silts alternate with sandy silts and silty sands	Clayey silts alternate with sandy silts and clayey–sandy silts
	✓	Poorly and very poorly sorted	Poorly sorted	Poorly and very poorly sorted
	✓	Similar mode values throughout the core and nearby cores. Common bi- and tri- modal values	Different mode values. Common uni- and bi-modal values	Different mode values. Common bi- and tri-modal values
Carb. Cont.	✓	Rich in carbonate content	Low carbonate content	Low to medium carbonate content
Sand Frac.	✓	Siliciclastic-bioclastic nature	Terrigenous nature	Terrigenous with presence of shell fragments
	✓	Shiny-angular and subangular quartz grains	Shiny-angular and subangular quartz grains	Matt, rounded and shiny subangular quartz grains
Ichnofabric	✓	Well-developed mottled silt background with fossil traces (C2, C3, C4)	Mottled background (Td)	Alternation of poorly-developed mottled and unmottled facies with a few trace fossils
	✓	Some trace fossils in homogenous muds infilled by silts from the overlying lithofacies (C1, C5)	Lack of mottled background and trace fossils (Te)	
Bulk XRD	✓	Rich in calcite	Rich in quartz	Rich in quartz
Clay XRD	✓	Rich in smectite with high S/I ratio values	Rich in illite with low S/I ratio values	Rich in illite with low S/I ratio values
S. Seq.	✓	Complete Stow & Faugères sequence (C1 to C5), common in Unit IA	Truncated Bouma sequence (Tc, Td, Te), common Td and Te divisions in upper part of Unit II	No specific textural vertical trend. Matrix-supported sediment with mud clasts and deformed beds
	✓	Truncated sequences (basecut-out) common in subunit IC	Grading toward top of sequence common in Tc	
	✓	Similar sequence thickness with internal gradational boundaries	Different thicknesses (thin to thicker) with sharp lower boundaries	Different thicknesses (thin to thicker)

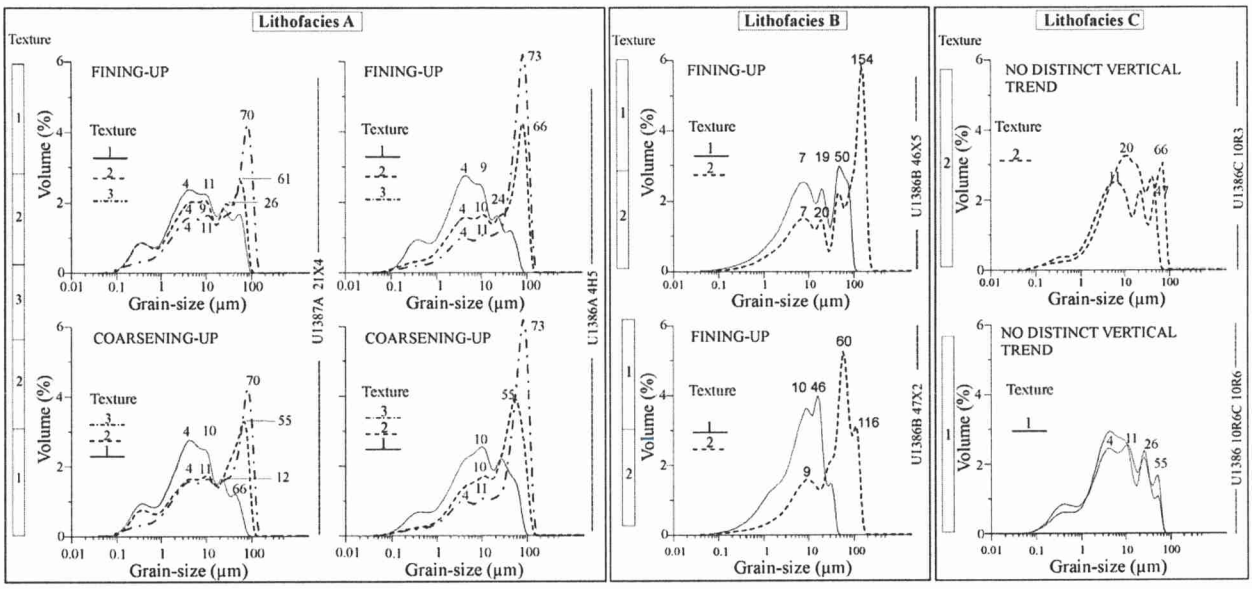

Fig. 3. Sedimentological description showing the granulometric parameter distribution and modes of lithofacies A (U1387A 21X4 and 4H5), lithofacies B (U1386B 46X5 and 47X2) and lithofacies C (U1386C 10R3 80 and 88 cm and 10R6 70 and 77 cm).

mottled background sediment with intercalations of unmottled sediments, generally found at the top of the very fine clayey-silt succession of textures (mean 3–10 μm), and also showing a few distinct trace fossils (green stars in Fig. 5 for traces infilled from host lithofacies); and 4) a lack of mottled background and trace fossils, typical in the homogeneous very fine clayey-silt (mean 6 μm) beds. Lithofacies C shows distorted stratified sediments and homogeneous sediments with mud clasts. The first is characterized by highly convoluted folded with colour-banded alternations of dark greenish-grey and greenish-black muds and the contacts between these beds are marked by truncations and zones of intense shearing (Fig. 4). The homogeneous mud appears as uniform mud matrix with small, soft mud and sand clasts. This lithofacies shows an alternation of poorly developed mottled and unmottled facies (number 5 in Fig. 5) with a few trace fossils (yellow and green stars for traces infilled from overlying and host lithofacies, respectively).

4.1.3. Carbonate content and sand fraction composition

Lithofacies A, with high carbonate content (18%–45%), is characterized by a mixed siliciclastic-bioclastic sand fraction composition. This fraction is dominated by biogenic components, mostly planktonic foraminifers (entire and fragments) with lesser quantities of others (e.g., benthonic foraminifers and ostracods), and quartz as a terrigenous component. The quartz grains are angular and subangular in shape (Fig. 6A). Lithofacies B, with low carbonate content (4%–19%), is characterized by a terrigenous sand fraction (80%–100%), mostly quartz (Fig. 6A). Some samples (e.g., intervals U1386B 47X1 99, 103, 108 and 115 cm; 48X2 13, 21 and 32 cm) also contain significant amounts of mica (up to 50%) and low percentages (<5%) of other components (e.g., glauconite, hornblende, and rock fragments). The quartz grains are angular and subangular in shape and show a prevalence of shiny surfaces (letters a and b in Fig. 6B). Lithofacies C displays low and moderate carbonate contents (4%–26%) and a heterogeneous sand fraction composition, being dominated by terrigenous components, particularly quartz (up to 95%) and also heterometric fragments of gastropods and other molluscs (Fig. 6A). The quartz grains are spherical and rounded and show prevalent matt faces with a polished surface (letters c and d in Fig. 6B).

4.1.4. Bulk mineral composition

The XRD analysis of the bulk fraction indicates that sediments are mainly composed of quartz, clay minerals, calcite and dolomite, with trace amounts of aragonite, microcline, albite, paragonite, and haematite. Lithofacies A, B and C show distinct variations between the major components of the bulk mineralogy, except for dolomite contents, which is more uniform (Fig. 7). Lithofacies A is richer in calcite (14%–32%), with highly variable quartz (9%–41%) and clay mineral (12%–41%) content, and a lower percentage of dolomite (5%–16%; Fig. 7A). There are two bulk mineral assemblages: i) quartz > calcite > clay minerals > dolomite, and ii) quartz > clay minerals > calcite > dolomite. In contrast, lithofacies B and C are richer in quartz (up to 58%) and have lower percentages of calcite (<19%; Fig. 7B). Specifically, lithofacies B is richer in quartz (22%–68%) and poorer in calcite (2%–20%), with a variable percentage of clay minerals (10%–46%) and a low dolomite content (2%–11%). Lithofacies C is also richer in quartz (22%–60%) and poorer in calcite (10%–18%), with great variations in the clay mineral content (18%–41%) and minor percentages of dolomite (5%–15%; Fig. 7B). Both lithofacies, B and C, show a quartz > clay minerals > calcite > dolomite bulk mineral assemblage.

4.1.5. Clay mineral composition

The XRD analysis of the clay fraction indicates that the sediments are mainly composed of illite, chlorite, kaolinite and smectite (Fig. 8). Lithofacies A, B, and C show variations in their major components, with the most significant clay mineral variations being between illite and smectite. Lithofacies A is poorer in illite (<39%) and richer in smectite (18%–33%), with higher values for the S + K/I + C (>0.8) and S/I (>0.6) ratios (Figs. 8 and 9). The dominant mineral assemblage is illite> > kaolinite > smectite > chlorite. Lithofacies B and C exhibit quite similar percentages of clay minerals. Both are richer in illite (37%–60%), reaching 73% in Lithofacies C, and poorer in smectite (0%–21%) with lower S + K/I + C (<0.8) and S/I (<0.6) ratios (Figs. 8 and 9). The mineral assemblage is illite ≫ kaolinite ≫ chlorite > smectite for Lithofacies B, and illite ≫ kaolinite > chlorite for lithofacies C. In addition to these clay minerals, several beds of lithofacies B contain two further minerals: i) magnesium-hornblende (intervals U1386B 47X2 23, 38, 56 and 64 cm; U1387B 47CC 3 cm, 48X2 129 and 147 cm, 48X3 9 and 14 cm); and ii) gypsum (intervals U1386B 47X1 115 and 117 cm).

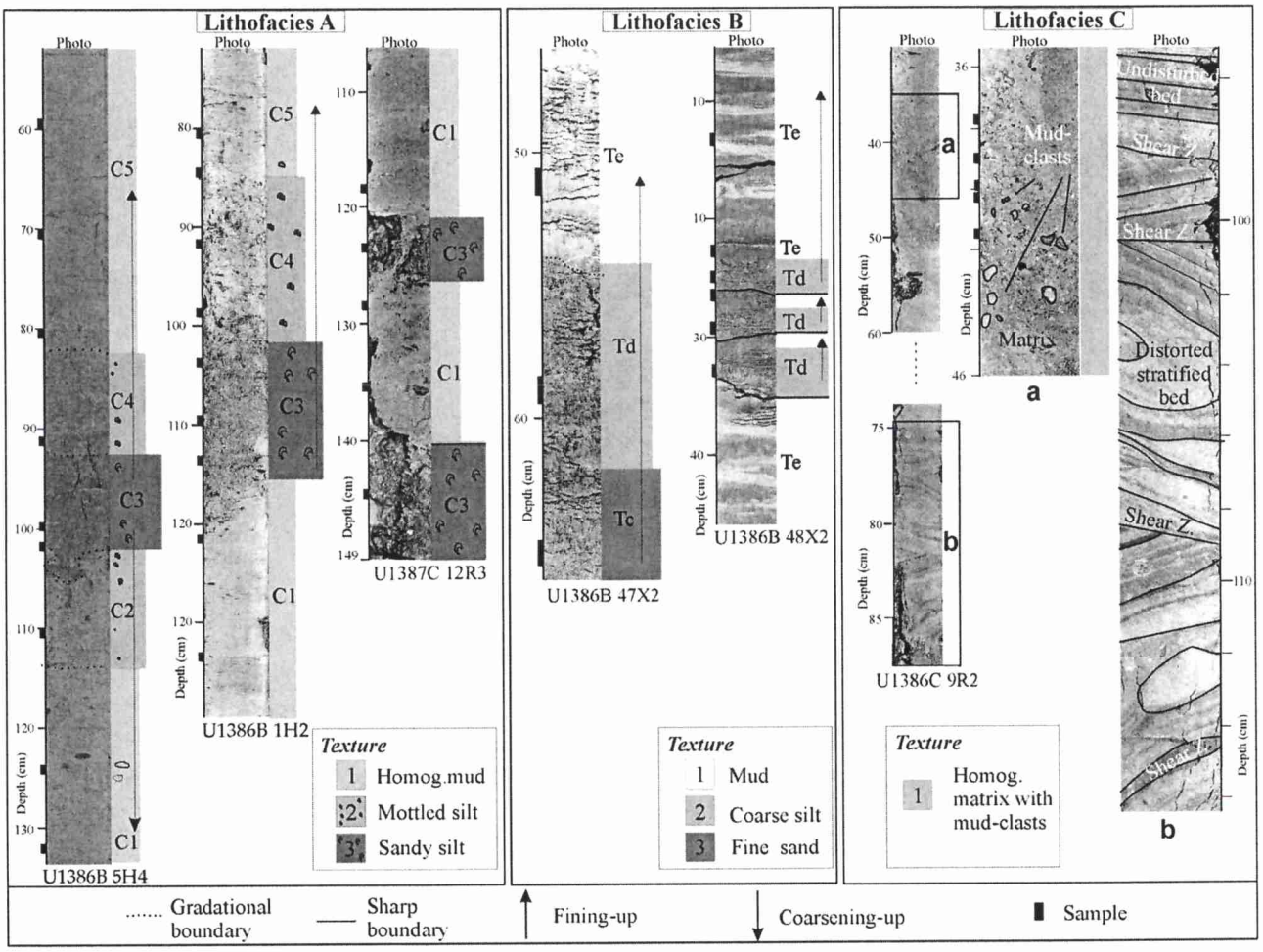

Fig. 4. Selected core photographs showing the main sedimentary sequences of the Pleistocene Faro Drift deposits. The sequences of lithofacies A display complete contourite sequence (C1 to C5) and truncated sequences (C3 to C5, and C3), the sequences of lithofacies B shows fining-up sequence; and the sequences of lithofacies C display a matrix with mud-clasts (a) and highly deformed beds (b). Legend: C1 to C5 refer to the contourite divisions of Stow and Faugères (2008); Tc, Td and Te are the turbidite divisions of the Bouma sequence; Homog. Homogeneous.

5. Discussion and conclusions

5.1. Genetic interpretation of lithofacies

The sedimentological and mineralogical attributes of lithofacies A, B and C making up the Pleistocene samples of Sites U1386 and U1387 provide significant clues for the genetic and environmental interpretations of the Faro Drift deposition. Each individual attribute is of little significance but when they are considered together interesting interpretative results are obtained. We are aware that the degree of accuracy is limited by the number of samples studied (149 samples), but dues to the great number of variables examined (~20) it is sufficient to discriminate between the principal sedimentary processes responsible for their deposition. Two major styles of sedimentary process are interpreted from Sites U1386 and U1387: i) alongslope processes controlled by bottom currents, and ii) downslope gravity-flow processes (turbidity currents, debris flows). Lithofacies A, dominant in Unit I, is the product of alongslope bottom currents. Lithofacies B, present in the upper part of Unit II, is interpreted as deposits originated by turbidity currents. Lithofacies C, presents also in the upper part of Unit II, is interpreted as a product of debris flows. We discuss below the principal criteria that have been most effective to distinguish between contourites and gravity-flow deposits.

5.2. Distinguishing criteria

5.2.1. Grain-size vertical trend and sedimentary structures

The classical contourite sequence was originally proposed by Gonthier et al. (1984) and Faugères et al. (1984) and it has been used as the standard facies model for interpreting deposition by alongslope processes in the deep sea (Viana et al., 1998; Toucanne et al., 2007; Mulder et al., 2013; Brackenridge, 2014). It comprises a bi-gradational sequence, with coarsening-up from homogeneous mud to mottled mud/silt to sandy silt/silty sand, followed by fining-up through the same facies succession in reverse order. This corresponds to the five sediment divisions (C1 to C5) of Stow and Faugères (2008). Facies sequences in lithofacies A are wholly consistent with the classical countourite sequence and partial sequences. Thus, the complete sequence formed by 1–2–3–2–1 textures corresponds to the five divisions C1 to C5. The truncated sequences formed mainly by 1–3–2–1 and 1–3–1 textures match to the divisions C1–C3–C4–C5 (fining upward), and C1–C3–C1 (Fig. 4). In addition, lithofacies A shows a general lack of primary sedimentary structures, poor and very poor sediment sorting and a relatively high level of mixing by bioturbation. Similar features have also been recognised as characteristic for other fine-grained contourite deposits (Stow et al., 1986, 2002; Brackenridge, 2014; Rebesco et al., 2014).

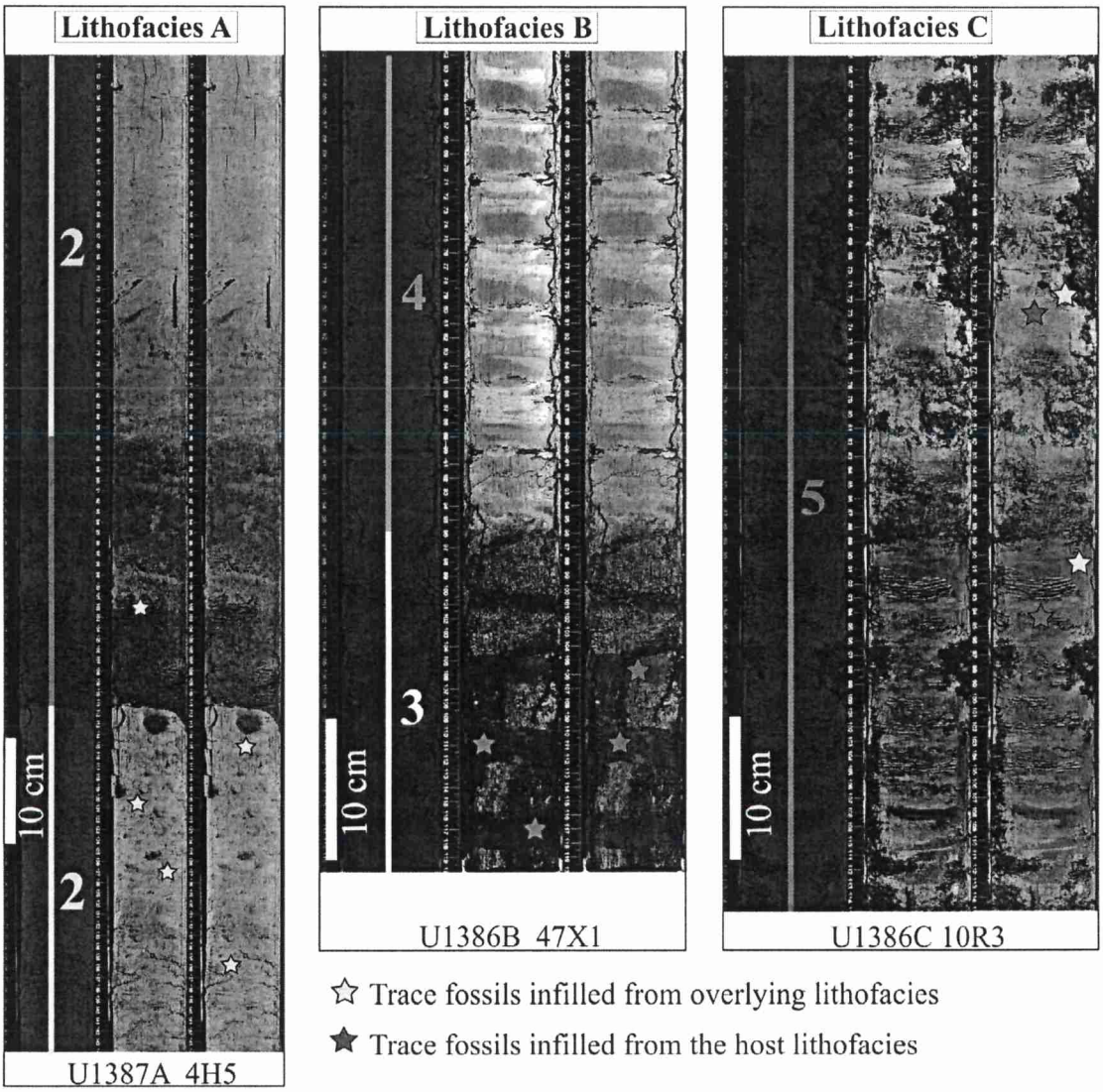

Fig. 5. Selected original core photographs and digital image treatment of lithofacies A, B, and C from the Pleistocene Faro Drift deposits showing five ichnofabric (1 to 5): 1) well-developed mottled background; 2) homogenous muds with some trace fossils infilled by relatively coarser sediments; 3) well-developed mottled background with unmottled intercalations and few trace fossils; 4) no mottling and no trace fossils, and 5) alternation of thick, poorly developed mottled and unmottled deposits with few trace fossils.

The grain-size variations noted (complete and partial bi-gradational sequences) can be broadly linked to variations in bottom current velocity (McCave and Carter 1997; Mulder et al., 2006; Toucanne et al., 2007; Stow and Faugères, 2008) and to changes in sediment provenance (Brackenridge, 2014; Rebesco et al., 2014). Bottom current variability of the MOW can be due to its interaction with local topography and/or different oceanographic processes (baroclinic and barotropic internal waves) (Kenyon and Belderson, 1973; Ambar and Howe, 1979; Baringer and Price, 1997; Llave et al., 2006; Stow et al., 2013), and also due to the upper and lower MOW core location changes. These latter changes may be linked to glacial and interglacial climate cycles and/or to millennial-scale oceanographic cycles (Llave et al., 2006; Toucanne et al., 2007; Hernández-Molina et al., 2014). Therefore, those sequences could be explained by the changing transport capacity of MOW and depositional mechanisms (suspended vs. bed load). The complete sequences (C1 to C5) are related to long-term changes in bottom-current velocity. The dominant middle-to-top sequences reflect the gradual onset in deposition after a period of erosion, according the model of Stow and Faugères (2008). With respect to grain-size variations linked to changes in sediment provenance, we discard this option because our sediment analysis results suggest the lack of changes during the Pleistocene, at least in the analysed samples, as will be discussed below (Section 5.2.3).

The classical turbidite sequence, was proposed by Bouma (1962) and has been commonly used as the standard interpretative facies model for the deposits of turbidity current (Shanmugam, 1997). A turbidite sequence is defined by five divisions (Ta to Te) and is the result of deposition from a single turbidity-current. Complete sequences are rare, and partial sequences are the norm (Walker, 1965; Alonso and Maldonado, 1990; Alonso et al., 1996, 1999, 2008; Talling et al., 2004; Gervais et al., 2006). In the lithofacies B, such sequences with normal grading and the presence of some sedimentary structures may be attributed to Tc, Td, Te divisions (Fig. 4). The beds fine upwards from sharp and erosional basal contacts. Also common are graded silt-laminated beds that show sharp and erosional basal contacts for the silt laminae, but relatively little grain-size difference between mud (mean 8 μm) and silt (mean 11 μm) laminae. This facies can be attributed to the standard sequence of fine-grained turbidites of Stow and Shanmugam (1980).

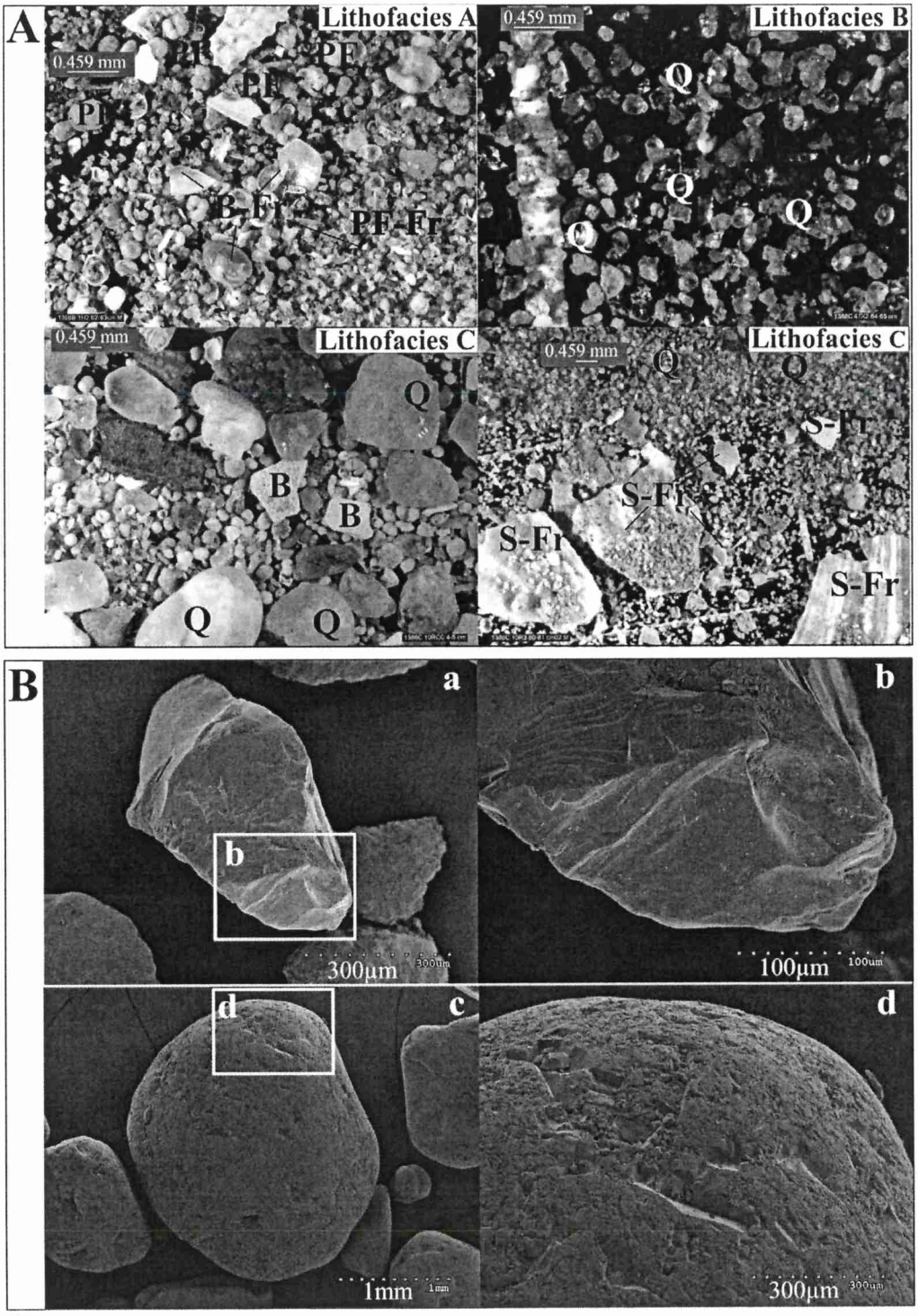

Fig. 6. Images of the sand fraction components of the Pleistocene Faro Drift deposits: A) binocular microscope photos showing the main components of lithofacies A, B and C; B) SEM microphotographs showing the morphoscopic features of quartz grains, in which a) and b) are shiny, angular and subangular quartz grains (e.g., interval U1386B 47X2, 38–39 cm) and c) and d) are matt, rounded and subrounded quartz grains (e.g., interval U1386C 10RCC, 4–5 cm). Legend: Q, quartz; B-Fr, biogenic fragments; PF, planktonic foraminifera; PF-Fr, planktonic foraminifera fragments; S-Fr, shell fragments.

Some turbidites show very poor sorting throughout. These have been recognised by various authors (e.g., Piper, 1973; Zaho et al., 2011). Piper (1973) explains the poor sorting of turbidites by deposition from rapid cohesion deposition of clay, trapping silt-size particles in the head of turbidity current. Although in a discrete beds, the poor sorting of Td division could be explained by the bioturbation structures sometimes found at their tops (Fig. 5). Bioturbation causes remobilization of the silt and its contamination with the finer overlying sediments as have also been observed in fine-grained turbidite sequences of African continental margin (Wetzel, 2007).

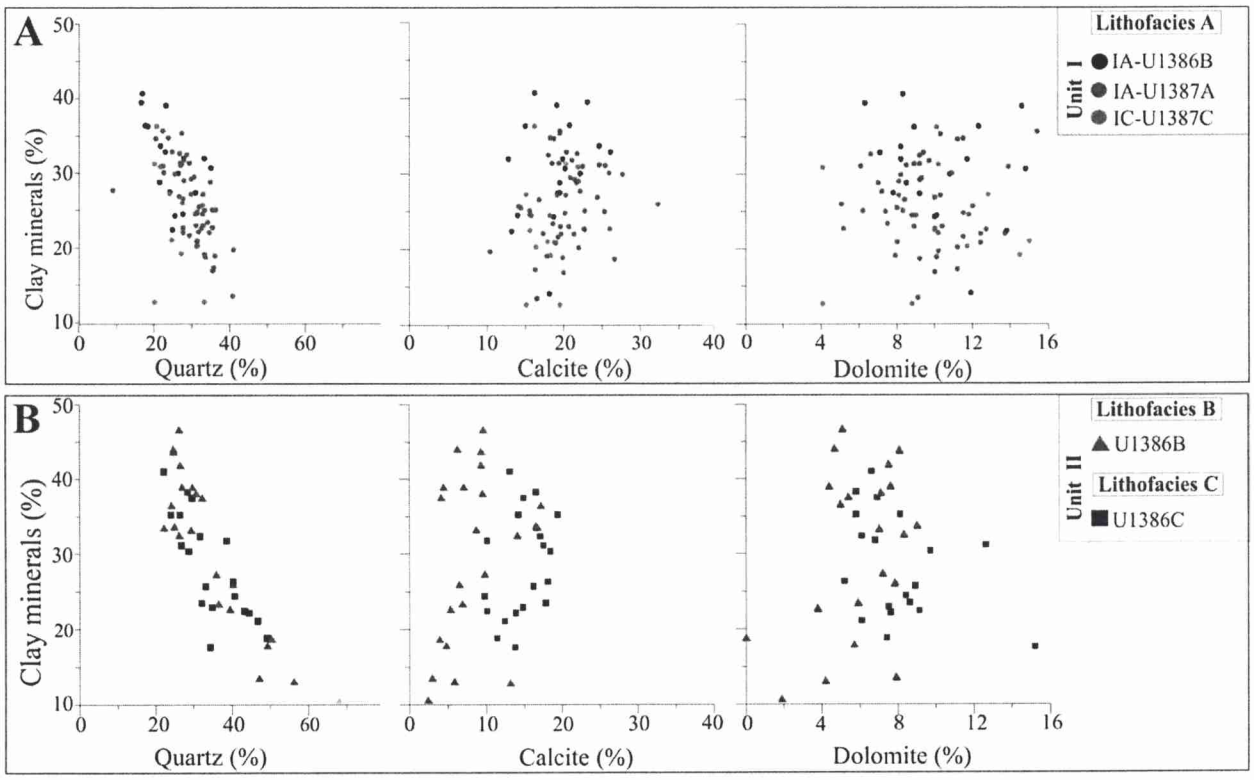

Fig. 7. Bulk mineralogy of the Pleistocene Faro Drift deposits showing the binary plots of clay minerals vs quartz, vs calcite, and vs dolomite for lithofacies A in Unit I from Hole U1386B and Holes U1387A,C and for lithofacies B and C in the upper part of Unit II from Holes U1386B,C.

Mass-transport deposits (slides, slumps and debrites) are recognised within cores on the basis of their disorganized and chaotic sedimentary structures (Almagor and Schilman, 1995; Nardin et al., 1979; Jenner et al., 2007; Tripsanas et al., 2008; Ratzov et al., 2010). In this study, we interpreted the occurrence of cohesive debris flows as explaining the deposition of those homogeneous matrix-supported mud-clast beds (U1386B 9R2-letter a in Fig. 4) and shear deformational structures (U1386B 9R2-letter b in Fig. 4) that characterize lithofacies C. Similar

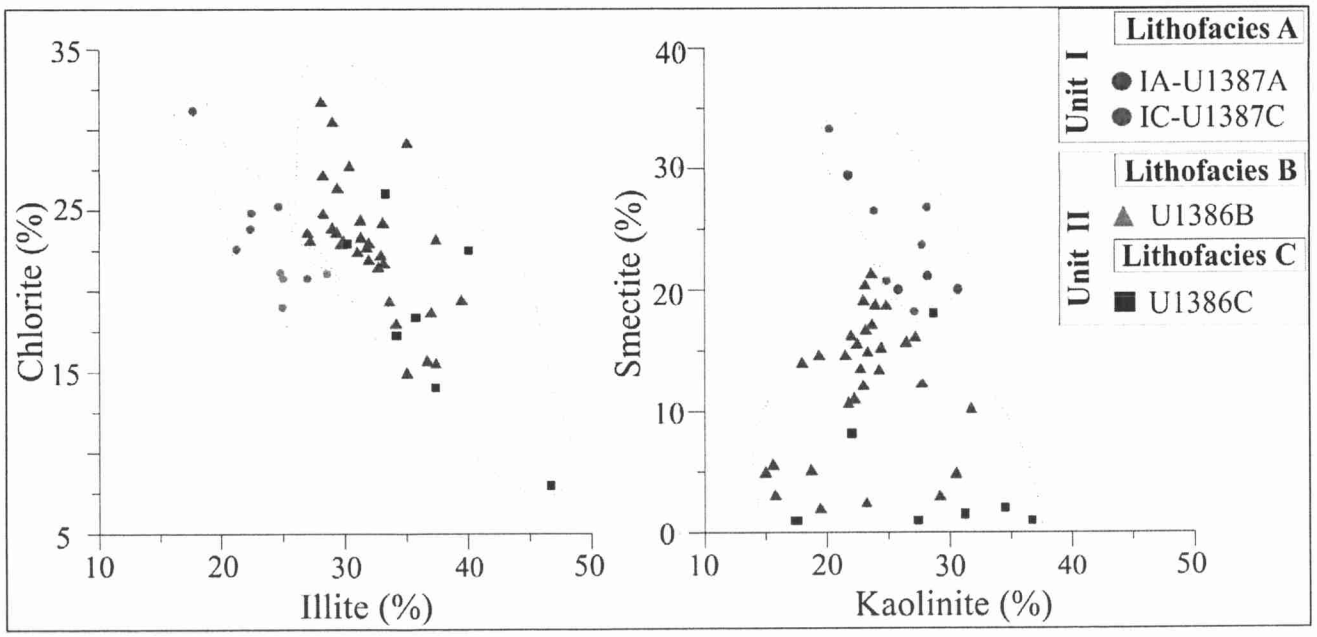

Fig. 8. Clay mineralogy of the Pleistocene Faro Drift deposits showing the binary plots of chlorite vs illite, and smectite vs kaolinite for the lithofacies A (Unit I, U1387A,C), and lithofacies B and C (upper part of Unit II – U1386B,C).

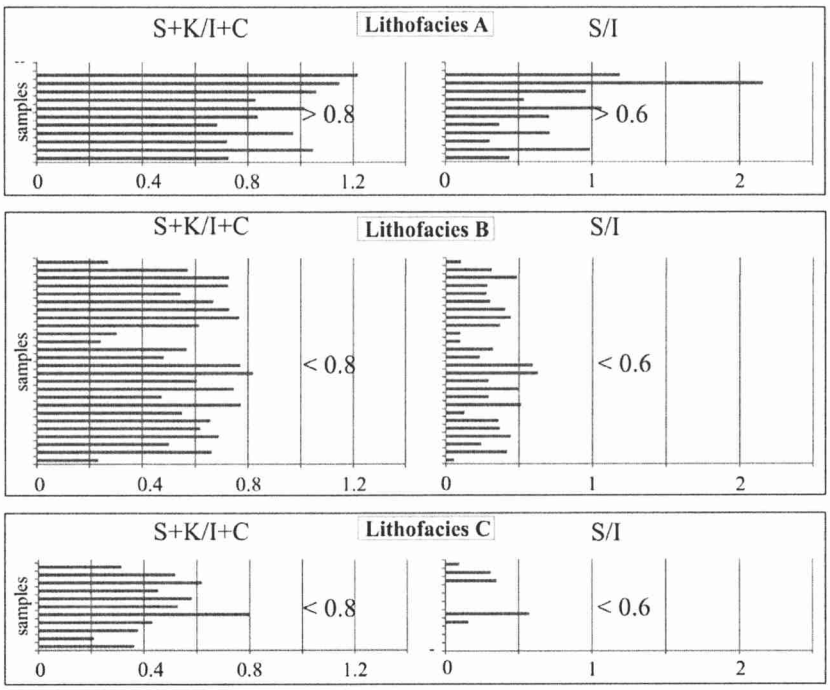

Fig. 9. Smectite + kaolinite/illite + chlorite ratio (S + K/I + C) and smectite/illite ratio (S/I) of the Pleistocene Faro Drift deposits for lithofacies A, B and C.

sedimentary structures, grain-size pattern and sand fraction composition were described by Ducassou et al. (2016) in debrites (D4) overlying the Early Pleistocene at Site U1386.

5.2.2. Modal frequency distribution

This criterion is useful to understand the pattern of sediment transport because it can help to decipher the complex interaction between the sediment source and MOW hydrodynamic flow behaviour along slope in the Gulf of Cadiz (Folk and Ward, 1957; Rea and Hovan, 1995). In the Faro Drift, the modal frequency distribution is significantly different between the contourites and gravity-flow facies (turbidites and debrites). For contourites, the bi- and tri-modal sediments have similar values and only the relative proportions of the modes vary through a contourite sequence, as well as in different locations across the drift. This means that the mode values are nearly constant through the different textures that make up the sequences, and that steady conditions of supply are maintained over time.

The dominant mode values are mostly in the silt grain-size range, which indicates that this is the dominant "background" component of the Faro Drift. The modal constancy between nearby contourite sequences must reflect the prevalence of a bottom current that is strong enough to move silt-sized particles and whose variations in energy levels produce variations in their relative proportions. On the other hand, the bi- and tri-modal signatures suggest two or three dominant sediment components as well as the break-up of clay flocs prior to grain-size analysis.

In contrast, turbidites and debrites have variable mode values throughout their sequences. We suggest that this fact is mainly controlled by the through mixing of components from allochthonous source areas and their transport by gravity-driven downslope processes. In most cases there appears to have been little interaction with the "background" bottom current conditions. The biogenic sand fraction of debrites (fragments of bivalves and gastropods) is consistent with a continental shelf origin of this part of the sediment. Likewise, the mode differences between nearby turbidite and debrite sequences would be explained because those turbidity and debris flow processes originated from different areas and/or had different rheology.

5.2.3. Sediment composition and provenance

Literature shows examples of the inferences derived by sedimentologists from the present day position of continental sediment sources to the mineral composition (clay and bulk mineralogy) in the sea-floor and subbottom sediments of deep sea areas (Weaver and Rothwell, 1987; Chamley, 1989; Pearce and Jarvis, 1992; Martínez-Ruíz et al., 1999; Hoogakker et al., 2004; Frenz et al., 2009; Wynn et al., 2012), although their transport and deposition may have taken place in lowered sea-level conditions when river mouths were closer to the continental slope (Miall, 1991). In this work, we use mineralogical composition (clay and bulk mineralogy) as indicators to establish the potential source of sediments coming from the surrounding soils and geological formations of the fluvial drainage basins surrounding the Gulf of Cadiz (Guadalquivir, Tinto-Odiel and Guadiana rivers). Previous studies of surficial coastal and shelf deposits allowed the identification of different fluvial sources, the Guadiana plus Tinto-Odiel source on one side and the Guadalquivir source on the other side (Grousset et al., 1988; Vergnaud-Grazzini et al., 1989; Gutiérrez-Mas et al., 1995; López-Galindo et al., 1999; Lobo et al., 2001; Gutiérrez-Mas et al., 2003; Maldonado et al., 2003; González et al., 2004; Achab and Gutiérrez-Mas, 2005; Machado et al., 2005; Rosa et al., 2013). In addition, the submarine depositional bodies formed mostly by their sediment supply during the different stages of sea-level can be demarcated in the Quaternary sedimentary register (Lobo et al., 1999). In the Faro Drift, the clay minerals are detrital rather than authigenic in origin, as suggested by the young age (Pleistocene) of the sediments, precluding significant diagenetic change, as well as the fact that they typically contain a large amount of intermixed illite species in the continental shelf (Gutiérrez-Mas et al., 2003). Furthermore, we can assume that drainage areas and patterns did not vary greatly through the Quaternary and there has not been a significant mixing process masking the local mineral signatures during the glacio-eustatic sea-level changes, at least at scale of the two major sources noted above.

Although the mineral composition of the clay and bulk fractions alone can be used as indicative of provenance (Chamley, 1989; Martínez-Ruíz et al., 1999; Machado et al., 2005), here we complement it with sand fraction components. The amount and characteristics of the

sand fraction components allow discrimination between contourites and gravity-facies and their sediment source. Grain-shape, roundness and surface texture analysis of quartz grains are also used to infer processes seen in modern coastal and shelf environments and hence can be indicative of provenance (Gutiérrez-Mas et al., 2003; Moral Cardona et al., 2005). Detrital muscovite mica is a common terrigenous component resistant to degradation during the transport. During the transport and deposition, only micas of smaller grain-size could have been degraded (Martínez-Ruíz et al., 1999). In our samples, degradation is not significant, and micas from all samples are very well preserved, which supports their origin by physical weathering of the outcropping metamorphic rocks.

5.2.3.1. Clay mineral approach. The differences in clay minerals between contourites and gravity-flows facies (turbidites and debrites) can be attributed to their different sources. For contourites, we propose that their clay mineral assemblage (illite ≫ kaolinite > smectite > chlorite) with the notable presence of smectite (18%–33%) and interstratified illite–smectite (I–S) has one primary potential source, the Guadalquivir River. This assemblage is similar to the association observed in the Neogene and Quaternary rocks of the Bay of Cadiz and Guadalquivir Basin, and in the terraces of the Guadalete River, as reported by Gutiérrez-Mas et al. (1995), who suggested the Guadalquivir River as the main source area for these clay minerals (Fig. 10). This interpretation is also supported by Mélières (1974); López-Galindo et al. (1999) and Machado et al. (2005), who obtained high contents of smectite and the presence of interstratified I-S, at the Guadalquivir river mouth and in its prodelta sediments, decreasing toward the shelf but increasing on the Cadiz upper continental slope. These higher smectite quantities contrast with the low values found in other nearby prodeltas of the eastern Gulf of Cadiz, which also decrease toward the shelf (Fernández-Caliani et al., 1997; López-Galindo et al., 1999; González et al., 2004; Machado et al., 2005). These high smectite quantities contrast with the low values found in other nearby prodeltas of the easternmost and western of Gulf of Cadiz (Machado et al., 2005).

In addition to the Guadalquivir River, we propose the nearby Alboran Sea in the Mediterranean Sea as a complementary source region and transport by the MOW (Fig. 10). In this case, the smectite would have been transported by the surficial AW eastward into the Alboran Sea and back again into the Atlantic by the MOW, being deposited along the Iberian continental slope and mimicking the trajectory of the MOW, as was already suggested by Grousset et al. (1988); Vergnaud-Grazzini et al. (1989) and López-Galindo et al. (1999). This mechanism could explain the otherwise anomalous increase of smectite on the Cadiz upper continental slope deposits (Mélières, 1974; López-Galindo et al., 1999) compared with lower values on the continental shelf. Our results (Fig. 8) with S + K/I + C (>0.80) and S/I (>0.5) ratio values are comparable to those (S + K/I + C ratio, 0.64–0.85; S/I ratio, >0.5) in the Gulf of Cadiz and even off the Cap St Vincent. In fact, mineralogical clay evidence of this complementary source may be found as far north as Lisbon where the presence of smectites (~20%) has been also detected (Vergnaud-Grazzini et al., 1989). The remarkable uniformity in clay mineralogy of contourites observed in Fig. 7 indicates a common and stable sediment source. This would be achieved by significant mixing and long-distance transport within the MOW. To confirm this interpretation we consider it necessary to examine, using the same approaches applied in this work, the other three sites (U1388, U1389, and U1390) drilled in the Gulf of Cadiz, and the two sites (U1385 and U1391) drilled off the West Iberian margin during Expedition 339.

For gravity-flow deposits a different sediment provenance is proposed. The clay mineral assemblage of both facies, turbidites and debrites (illite < <kaolinite > chlorite > smectite) with enrichment of illite (up to 73%) and impoverishment of smectite (0%–15%) point to the primary source being the Guadiana River and Tinto-Odiel rivers, which drain metamorphic and igneous rocks (Iberian Massif) and deposit their sediment load on the continental shelf (Morales, 1997; González et al., 2004). This interpretation is supported by the enrichment in illite, chlorite, and kaolinite, and the little or no smectite in the continental shelf sediments in front of these rivers. Additional clay mineralogical evidence, such as the occurrence hornblende in several turbidite samples (e.g., intervals U1386B 47X2, 56 and 64 cm; 47XCC, 3 cm; 48X2, 129 and 147 cm; 48X3, 9 and 12 cm), also supports this interpretation. The hornblende represents an amphibole coming from metamorphic rocks that outcrop in the Guadiana River drainage basin (Vidal et al., 1993). The presence of gypsum (intervals U1386B 47X1, 115 and 117 cm) that has also been detected in the overlaying debrite 4 of Ducassou et al. (2016), could be explained either as detrital, from the Tinto-Odiel river flood plains, or as an authigenic mineral formed on the shelf by the reaction of the carbonate biogenic material with acid sulphate water (Siesser and Rogers, 1976; Fernández-Caliani et al., 1997).

5.2.3.2. Bulk mineral composition and sand fraction approach. For the contourites, the greater abundance of calcite (28% on average) quantified on the bulk fraction is proportionate to the high carbonate content of the total sample (18%–45%). It can be linked to the presence of biogenic components, mainly nannofossils and planktonic foraminifera. A second and additional potential source of calcite would be related to the presence of detrital carbonate in the sand fraction sourced from the marl-rich diapirs of the eastern upper slope in the Gulf of

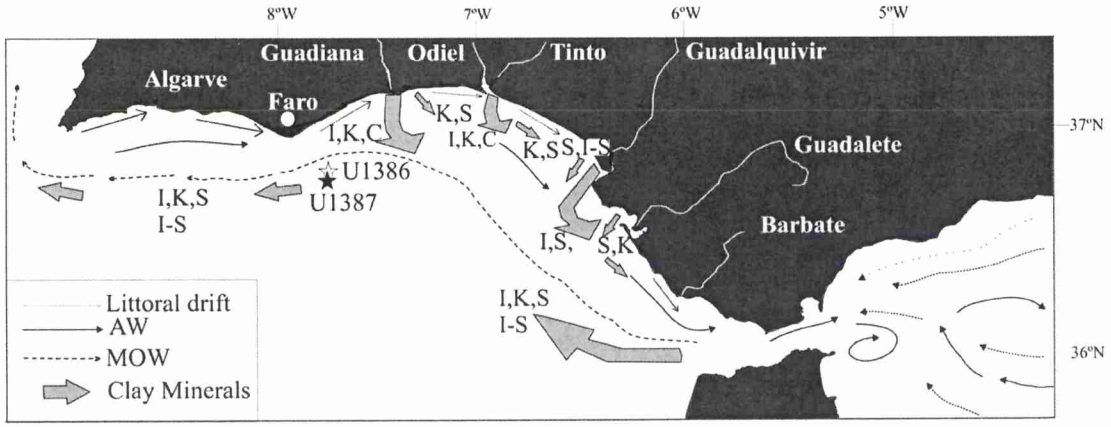

Fig. 10. Schematic map illustrating the main sedimentary sources of clay minerals and transport paths to the Faro continental slope. Characteristics are summarized from both previous works (López-Galindo et al., 1999; Machado et al., 2005) and the present work. Arrows size is proportional to the quantity of clay minerals (I, illite; S, smectite; K, kaolinite; C, chlorite, I-S interstratified illite-smectite). Legend of water masses in Fig.1.

Cadiz. These diapirs, which contain carbonate (15%–60%) (calcite, dolomite and aragonite) with variable proportions of quartz (17%–45%) and clay minerals (<35%) (Mhammedi et al., 2008), are eroded and the particles transported by the MOW (Nelson et al., 1999). The higher content of dolomite (>12%, Fig. 6A) in several samples of mud and sand-silt contourites versus samples of turbidites should support this hypothesis. The dominant source of quartz is most likely the Guadalquivir River, as this river drains metamorphic and sedimentary regions of the Betic Cordillera and Postorogenic Neogene materials supplying the greatest concentration of quartz detected near its mouth (López-Galindo et al., 1999), much of which is subangular with low sphericity and smooth surfaces (Figs. 1, 9). All these attributes are found in the sand fraction. Other possible sediment source could be in input from the Guadalete River, the mouth of which is situated within Cadiz Bay, and the Barbate River, located to the south of the study area. Even so, this source is not considered to have provided sediment for the contourites due to the different natures of quartz found in the contourites and the sediments supplied by this river. The Guadalete River injects sediment originating from erosion of the Aquitanian Numidic sandstone (Aljibe Sandstone), which contains very well-rounded quartz grains (Gutiérrez-Mas et al., 2003) contrasting to the angular-subangular quartz grains observed in the contourites.

For gravity-flow deposits the source area of quartz is probably the sequence of Palaeozoic metaschists and greywackes which are drained by the Guadiana River and Tinto-Odiel rivers which have very close drainage basin (Achab and Gutiérrez-Mas, 2005; Machado et al., 2005). This interpretation is supported by two clues given by the sand fraction: the shiny angular quartz in turbites, the dominant rounded shape displayed by quartz grains in debrites (Fig. 9B), and the abundance of micas in several turbidite samples. The shiny angular-subangular quartz of the turbidites may preferentially have come from the Guadiana shelf sediments based on the greater quantity of shiny angular-subangular quartz found in the river mouth there. In contrast, rounded matt quartz found in the debrites could be related to the Tinto-Odiel shelf sediments, considering the elevated content of round matt quartz grains in the Tinto-Odiel system. Mica particles of continental origin are linked to discharges from Guadiana, which give specific depositional imprint on the shelf sediments (González et al., 2004). The very high mica content (up to 70%) recognised in the sand fraction in some turbidite samples suggest that these components could be linked to discharge from the Guadiana and Tinto-Odiel rivers (Vidal et al., 1993). These rivers mainly drain metamorphic and igneous rocks and deposit their sediment load on the continental shelf. The high quantities of mica in front of these rivers contrast with its scarcity on the continental shelf off the Guadalquivir River (González et al., 2004; Achab and Gutiérrez-Mas, 2005). The traces of hornblende identified in the bulk mineralogy also support this interpretation because this mineral is present in the metamorphic rocks of the Guadiana River drainage basin (Vidal et al., 1993). In addition, the biogenous components of the sand fraction (ostracods, bivalves, gastropods) also suggest a shallow water environment deposition for the components of the debrites before the seafloor failure. A similar interpretation has also been suggested for the source of the overlying terrigenous debrites (D4) described by Ducassou et al. (2016).

To summarise, these approaches to interpretation of sediment provenance for the different lithofacies reflect different modes of long- and short-distance transport. According to the drainage basins here considered, most of the terrigenous sediment of contourites is coming from the distant Guadalquivir drainage basin whereas the terrigenous and biogenic components of turbidites and debrites are sourced more directly from vicinity fluvial drainage basins (Guadiana, Tinto-Odiel) close to the Faro Drift. Based on these observations and taking into account that mineral provenance is well constrained and lacks of significant mixing processes as it has been mentioned above, we therefore favour an interpretation that particles stripped off the distant Guadalquivir shelf margin delta by MOW fed primarily into the Faro Drift during the Pleistocene (Unit I-Holes U1386B, and U1387A,C); and the terrigenous particles of turbidites and debrites are injected downslope by gravitational processes especially during the Early Pleistocene (upper part of Unit II-Holes U1386B,C). The well preserved local mineralogical signature of their deposits also suggests that the gravity-flow processes are not significantly influenced by the MOW action. Alternatively, their fine suspended loads may be stripped off by the MOW and advected westward, away from the Faro Drift.

5.3. Depositional architecture of Pleistocene Faro Drift

The spatial and temporal distribution of the Pleistocene contourites, turbidites and debrites in combination with the seismic character and evolution of the Faro Drift (e.g., Hernández-Molina et al., 2014; Fig. 1C), allow us to define a preliminary model of the facies distribution. Further work will help confirm or refine this interpretation. Most authors have emphasised the role of geostrophic bottom currents in shaping the continental slope of Cadiz (e.g., Nelson et al., 1999; Mulder et al., 2003) but mass wasting and turbidity currents also occur locally, as was mentioned recently by Hernández-Molina et al. (2014) and Ducassou et al. (2016).

The lithofacies defined in this study characterize two drift domains, which were seismically defined by Stow et al. (2013) and Hernández-Molina et al. (2014): the palaeo-moat and drift domains (Figs. 1A and 10). The palaeo-moat deposits of the Early Pleistocene (1.66–1.9 to 1.24–1.27 Ma; Expedition 339 Scientists, 2012) are more strongly influenced by gravity-controlled deposition and ~50 m thick of gravity-flow deposits at Site U1386 could have been channelized by the palaeo-moat. Its duration should be strongly dependent of the sediment supply from the continental shelf as suggested by the stacked vertical succession of siliciclastic fine and coarse-grained turbidites interbedded with siliciclastic muddy debrites (number 2 in Fig. 11). Turbidite sequences are incomplete, mainly Td–Te sequences (fine-grained turbidites), and are characterized by their homogeneity in siliciclastic composition (mainly quartz), erosive lower boundary, lack of primary sedimentary structures, and mottled appearance in some beds. Based on palaeoenvironmental and sequence stratigraphy studies in the area (González et al., 2004; Roque et al., 2012; Hernández-Molina et al., 2013, 2014; Stow et al., 2013; pers. comm. P. Lobo), these gravity flows were probably funnelled by fluvial-fed small canyons related to the Guadiana and Tinto-Odiel rivers, as suggested by the bulk and clay mineralogical composition. Taking into account sequence stratigraphic (Llave et al., 2002; Hernández-Molina et al., 2002; Llave et al., 2007a, b; Roque et al., 2012) and structural (Medialdea et al., 2004) studies in the Gulf of Cadiz, gravitational processes took place primarily during sea-level fall and lowstand stages when the Guadiana plus Tinto-Odiel river mouths were located close to the shelf-break, and the occurrence of gravity-driven instability processes is significant because deposition occurs on the steeper continental slope (Chiocci et al., 1997), and/or could be triggered by tectonic pulses.

The drift deposits recorded from the Early to Late Pleistocene are quite different from those of the palaeo-moat domain (Fig. 11), here the contourite construction represents the largest part of the total volume of accumulated sediment on the Faro Drift during this time. There is also relatively high sedimentation rate (up to 35 cm/ky) of contourite deposits and enhanced permanent activity of the MOW (Expedition 339 Scientists, 2012). The drift deposits are defined by a vertical succession of sandy, silty and mud contourite sequences, with homogeneity in the mixed siliciclastic-bioclastic nature, gradational boundaries, mud with lenses of coarse material, and a well-developed mottled background with trace fossils (number 1, 3, and 4 in Fig. 11). By contrast, the sequences are heterogeneous: basecut-out contourite sequences predominate during the Early and Middle Pleistocene, whereas the complete sequences develop during the Late Pleistocene (U1387A 4H5, 12X4) (Fig. 11). This heterogeneity in the vertical successions is the consequence of the general lateral migration of the

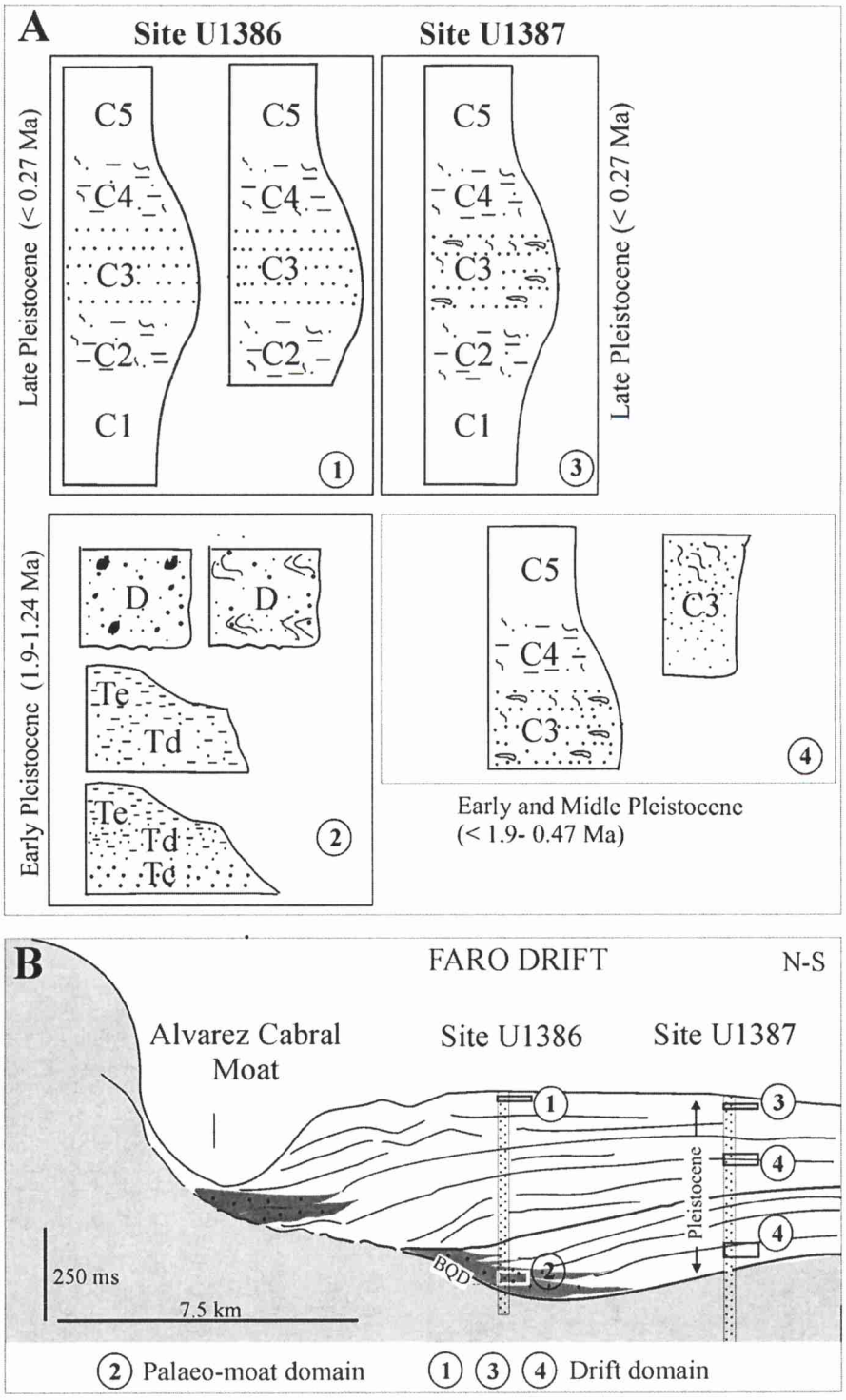

Fig. 11. Schematic representation of facies model for the depositional architecture of the Faro Drift deposits showing: A) the sedimentary sequences commonly encountered in palaeo-moat domain (number 2) and drift domain (numbers 1, 3, and 4) at Sites U1386 and U1387 during the Early, Middle and Late Pleistocene; and B) the Quaternary stratigraphic section showing the drift domains and the location of both studied sites and units based on the seismic profile of Fig. 1C. Legend: C1 to C5 refer to the contourite divisions. Tc, Td and Te correspond to the turbidite Bouma divisions; BQD, Lower Quaternary seismic reflector.

drift-moat system, as is reflected by its seismic architecture defined previously by Stow et al. (2013) and Hernández-Molina et al. (2014). The basecut-out contourite sequences occur in environments closer to the Alvarez Cabral moat (e.g., the internal side of the drift) and are being overlain by the complete contourite sequences deposited in a more distal drift environment (e.g., the external face of the drift). Therefore, basecut-out sequences occur where higher energy bottom currents and/or variations in sediment supply are more prevalent.

Acknowledgements

This study used samples and data collected through the Integrated Ocean Drilling Program (IODP). The research was supported through the MOWER (CTM 2012-39599-C03), MONTERA (CTM2009-14157-C0-02) and CGL2012-33281 projects funded by the Spanish Ministry of Economy and Competitiveness. The authors thank TGS-NOPEC for the use of the seismic profile on Fig. 1. We are grateful for the financial support of the CSIC10-4E-141 Project and the European Regional Development Fund for the acquisition of an XRD diffractometer (Instituto de Ciencias de la Tierra "Jaume Almera"-CSIC, Barcelona). Thanks also go to J. Elvira, who contributed to the processing and interpretation of the XRD diffractograms. We also wish to thank E. Vitorica and D. Parent for their assistance during sample preparation.

References

Achab, M., Gutiérrez-Mas, J.M., 2005. Nature and distribution of the sand fraction components in the Cadiz Bay bottoms (SE Spain). Rev. Soc. Geol. Esp. 18 (3–4), 133–143.

Almagor, G., Schilman, B., 1995. Sediment structures and sediment transport across the continental slope of Israel from piston cores studies. Sedimentology 42, 575–592.

Alonso, B., Maldonado, A., 1990. Late Quaternary sedimentation patterns of the Ebro turbidite systems (northwestern Mediterranean): two styles of deep-sea deposition. In: Nelson, C.H., Maldonado, A. (Eds.), The Ebro Continental Margin, Northwestern Mediterranean Sea. Mar. Geol. 95 (3/4), 353–378.

Alonso, E., Comas, M.C., Ercilla, G., Palanques, A., 1996. Data Report: textural and mineral composition of Cenozoic sedimentary facies off the western Iberian Peninsula, Sites, 897, 989, and 900. In: Whitmarsh, R.B., Sawyer, D.S., Masson, D. (Eds.), Proceedings of the Ocean Program, Scientific Results 149, College Station, TX (Ocean Drilling Program), pp. 741–754.

Alonso, B., Ercilla, G., Martínez-Ruíz, F., Baraza, J., Galimont, A., 1999. Pliocene–Pleistocene sedimentary facies at Site 976: depositional history in the northwestern Alboran Sea. In: Zhan, R., Comas, M.C., Klaus, A. (Eds.), Proceedings of the Ocean Drilling Program, Scientific Results 161, College Station, TX (Ocean Drilling Program), pp. 21–36.

Alonso, B., Ercilla, G., Casas, D., Estrada, F., Farrna, M., Garcia, M., Rey, D., Rubio, B., 2008. Late Pleistocene and Holocene sedimentary facies on the SW Galicia Bank (Atlantic NW Iberian Peninsula). Mar. Geol. 249, 46–63.

Alonso, B., Ercilla, G., Casas, D., Stow, D.A.V., 2014. Gravitative-vs-contourite facies: sedimentology and mineralogy of the Quaternary deposits of the Faro Drift (Gulf of Cadiz). In: Hernández-Molina, F.J., Stow, D.A.V., Llave, E., Roque, C., Sierro, G.J., Jiménez-Espejo, F., Sandoval, N. (Eds.), Mediterranean Outflow, 2 nd IODP 330 Post-Cruise Meeting, Tarifa (Cádiz, Spain), p. 72 (Abstract volume).

Alves, T.M., Gawthorpe, R.L., Hunt, D.W., Monteiro, J.H., 2003. Cenozoic tectono-sedimentary evolution of the western Iberian margin. Mar. Geol. 195 (1–4), 75–108. http://dx.doi.org/10.1016/S0025-3227(02)00683-7.

Ambar, I., Howe, M.R., 1979. Observations of the Mediterranean outflow: the deep circulation in the vicinity of the Gulf of Cadiz. Deep Sea Res. Part A 26 (5), 555–568.

Baringer, M.O., Price, J.F., 1997. Mixing and spreading of the Mediterranean outflow. J. Phys. Oceanogr. 27, 1654–1677.

Blott, S.J., Pye, K., 2001. Gradistat: a grain size distribution and statistics package for the analysis of unconsolidated sediments. Earth Surf. Landf. 26, 1237–1248.

Borrego, J., Morales, J.A., Pendón, J.G., 1995. Holocene estuarine facies along the mesotidal coast of Huelva, south-western Spain. In: Fleming, B.W., Batholomä, A. (Eds.), Tidal Signature in Modern and Ancient Sediments. International Association of Sedimentologists, Sp. Publ. 24, pp. 151–170.

Bouma, A.H., 1962. Sedimentology of some flysch deposits. A Graphic Approach to Facies Interpretation. Elsevier, Amsterdam (168 pp.).

Brackenridge, R.E., 2014. Contourite Sands in the Gulf of Cadiz: Characterisation, Controls and Wider Implications for Hydrocarbon Exploration. PhD. Heriot-Watt University, Institute of Petroleum Engineering (257 pp.).

Brackenridge, R.E., Hernández-Molina, F.J., Stow, D.A.V., Llave, E., 2013. A Pliocene mixed contourite-turbidite system offshore the Algarve Margin, Gulf of Cadiz: seismic response, margin evolution and reservoir implications. Mar. Pet. Geol. 46, 36–50.

Chamley, H., 1989. Clay Sedimentology. Springer-Verlag, Berlin, Heidelberg, pp. 163–190 (ISBN 3-387-50889-9).

Chiocci, F.L., Ercilla, G., Torres, J., 1997. Stratal architecture of Western Mediterranean margins as the result of the stacking of Quaternary lowstand deposits below "glacio-esutatic fluctuation base-level". Sediment. Geol. 112, 195–217.

Chung, F.H., 1974. Quantitative interpretation of X-ray diffraction patterns of mixtures. I. Matrix-flushing method for quantitative multicomponent analysis. J. Appl. Crystallogr. 7, 519–525.

Didon, J., Duran-Delg, M., Kornprobst, J., 1973. Homologies géologiques entre les deux rives du détroit de Gibraltar. Bull. Soc. Gén. Fr. 115, 77–105.

Dorador, J., Rodríguez-Tovar, F.J., 2014. A novel application of digital image treatment by quantitative pixels analysis to trace fossil research in marine cores. PALAIOS 24, 533–538.

Dorador, J., Rodríguez-Tovar, F.J., 2016. Stratigraphic variation in ichnofabrics at the "Shackleton Site" (IODP Site U1385) on the Iberian Margin. Paleoenvironmental implications. Mar. Geol. 377, 118–126.

Dorador, J., Rodríguez-Tovar, F.J., IODP Expedition 339 Scientists, 2014a. Digital image treatment applied to ichnological analysis of marine core sediments. Facies 60 (1), 39–44.

Dorador, J., Rodríguez-Tovar, F.J., IODP Expedition 339 Scientists, 2014b. Quantitative estimation of bioturbation based on digital image analysis. Mar. Geol. 349, 55–60.

Ducassou, E., Fournier, L., Sierro, F.J., Alvarez Zarikan, C.A., Lofi, J., Flores, J.A., Roque, C., 2016. Origin of the large Pliocene and Pleistocene debris flow on the Algarve margin. Mar. Geol. 377, 58–76.

Ercilla, G., Juan, C., Hernández-Molina, F.J., Bruno, M., Estrada, F., Alonso, B., Casas, D., Farran, M., Llave, E., García, M., Vázquez, J.T., D'Acremont, E., Gorini, C., Palomino, D., Valencia, J., El Moumni, B., Ammar, A., 2015. Significance of bottom currents in deep-sea morphodynamics: an example from the Alboran Sea. Mar. Geol. http://dx.doi.org/10.1016/j.margeo.2015.09.007.

Expedition 339 Scientists, 2012. Mediterranean outflow: environmental significance of the Mediterranean outflow water and its global implications. IODP preliminary report. p. 339. http://dx.doi.org/10.2204/iodp.pr.2012.

Faugères, J.C., Stow, D.A.V., 1993. Bottom-current controlled sedimentation: a synthesis of the contourite problem. Sediment. Geol. 82, 287–297.

Faugères, J.C., Gonthier, E., Stow, D.A.V., 1984. Contourite drift mounded by deep Mediterranean outflow. Geology 12, 296–300.

Fernández-Caliani, J.C., Ruiz Muñoz, F., Galán, E., 1997. Clay mineral and heavy metal distribution in the lower estuary of Huelva and adjacent Altantic shelf, SW Spain. Sci. Total Environ. 198, 181–200.

Fernández-Salas, L.M., Rey, J., Pérez-Vázquez, E., Ramírez, J.L., Hernández-Molina, F.J., Somoza, L., de Andrés, J.R., Lobo, F.J., 1999. Morphology and characterisation of the relict facies on the internal continental shelf in the Gulf of Cadiz, between Ayamonte and Huelva, (Southern Iberian Peninsula). Bol. Inst. Esp. Oceanogr. 15, 123–132.

Folk, R.L., Ward, W.C., 1957. Brazos river bar: a study in the significance of grain-size parameters. J. Sediment. Petrol. 27 (1), 327–354.

Frenz, M., Wynn, R., Georgiopoulou, A., Bender, V.B., Hough, G., Masson, D., Talling, P., Cronin, B.T., 2009. Provenance and pathways of late Quaternary turbidites in the deep-water Agadir Basin, northwest African margin. Int. J. Earth Sci. 98, 721–733.

Galindo-Zaldívar, A., Jabaloy, A., González-Lodeiro, F., Aldaya, F., 1997. Crustal structure of the central sector of the Betic Cordillera. Tectonics 16 (1), 18–37.

Garcia, M., Hernández-Molina, F.J., Llave, E., Stow, D.A.D., León, R., Fernández-Puga, M.C., Díaz del Río, V., Somoza, L., 2009. Contourite erosive features caused by the Mediterranean Outflow Water in the Gulf of Cádiz: Quaternary tectonic and oceanographic implications. Mar. Geol. 257, 24–40.

Garcia, M., Hernández-Molina, F.J., Alonso, B., Vázquez, J.T., Ercilla, G., Llave, E., Casas, D., 2015. Sub-circular depression structures and other erosive features at the Guadalquivir Bank Margin uplift, Gulf of Cadiz: interaction between bottom current, mass-wasting and tectonic processes. Mar. Geol. http://dx.doi.org/10.1016/j.margeo.2015.10.004 (in press).

Gervais, A., Mulder, T., Savoye, B., Gonthier, E., 2006. Sediment distribution and evolution of sedimentary processes in a small sandy turbidite system (Golo system, Mediterranean Sea): implications for various geometries based on core framework. Geo-Mar. Lett. 26, 373–395.

Gonthier, E.G., Faugeres, J.C., Stow, D.A.V., 1984. Contourite facies of the Faro Drift, Gulf of Cádiz. In: Stow, D.A.V., Piper, D.J.W. (Eds.), Fine-Grained Sediments: Deep Water Processes and Facies. Geological Society, London, Special Publications 15, pp. 275–292.

Gonthier, E., Faugères, J.C., Viana, A., Figuereido, A., Anschutz, P., 2003. Upper Quaternary deposits on the Sao Tomé Deep-sea channel levee system (South Brazilean Basin): major turbidite versus contourite processes. Mar. Geol. 199, 159–180.

González, R., Dias, J.M.A., Lobo, F., Mendes, I., 2004. Sedimentological and paleonvironmental characterization of transgressive on the Guadiana shelf (Northern Gulf of Cadiz, SW Iberia). Quat. Int. 120, 133–144.

Grousset, F.E., Joron, J.L., Biscaye, P.E., Latoucher, C., Treuil, M., Maillet, N., Faugères, F.C., Gonthier, E., 1988. Mediterranean outflow through the Strait of Gibraltar since 18,000 years B.P: mineralogical and geochemical arguments. Geo-Mar. Lett. 8, 25–34.

Gutiérrez-Mas, J.M., López-Galindo, A., González-Caballero, J.L., López-Aguayo, F., 1995. Las facies detríticas de la plataforma continental de Cádiz (tramo Chipiona-Trafalgar) en relación con la evolución de la dinámica sedimentaria reciente. Rev. Soc. Geol. Esp. 8 (1–2), 61–71.

Gutiérrez-Mas, J.M., Hernández-Molina, F.J., López-Aguayo, F.J., 1996. Holocene sedimentary dynamic evolution on the northern continental shelf of the gulf of Cádiz. Cont. Shelf Res. 16 (3), 1635–1653.

Gutiérrez-Mas, J.M., Moral, J.P., Sánchez, A., Domínguez, S., Muñoz-Pérez, J.J., 2003. Multicycle sediments on the continental shelf of Cadiz (SW Spain). Estuar. Coast. Shelf Sci. 57, 667–677.

Habgood, E.L., Kenyon, N.H., Masson, D.G., Akhmetzhanov, A., Weaver, P.P.E., Gardner, J., Mulder, T., 2003. Deep-water sediment wave fields, bottom current sand channels, and gravity flow channel-lobe systems: Gulf of Cádiz, NE Atlantic. Sedimentology 50 (3), 483–510. http://dx.doi.org/10.1046/j.1365-3091.2003.00561x.

Hanquiez, V., Mulder, T., Lecroart, P., Gonthier, E., Marchès, E., Voisset, M., 2007. High resolution seafloor images in the Gulf of Cádiz, Iberian margin. Mar. Geol. 246 (1), 42–59. http://dx.doi.org/10.1016/j.margeo. 2007.08.002.

Heimhofer, U., Adatte, T., Hochuli, P.A., Burla, S., Weissert, H., 2008. Coastal sediments from the Algarve: low-latitude climate archive for the Aptian–Albian. Int. J. Earth Sci. 97, 785–797.

Hernández-Molina, F.J., Somoza, L., Vázquez, J.T., Lobo, F., Fernández-Puga, M.C., Llave, E., Díaz-del Río, V., 2002. Quaternary stratigraphic stacking patterns on the continental shelves of the southern Iberian Peninsula: their relationship with global climate and paleooceanographic changes. Quat. Int. 92, 5–23.

Hernández-Molina, F.J., Llave, E., Somoza, L., Fernández-Puga, M.C., Maestro, A., León, R., Medialdea, T., Barnolas, A., García, M., Díaz del Río, V., Fernández-Salas, L.M.,

Vázquez, J.T., Lobo, F., Alveirinho Dias, J.M., Rodero, J., Gardner, J., 2003. Looking for clues to paleoceanographic imprints: a diagnosis of the Gulf of Cádiz contourite depositional systems. Geology 31 (1), 19–22. http://dx.doi.org/10.1130/0091-7613(2003)031<0019:LFCTPI>2.0.CO2.

Hernández-Molina, F.J., Llave, E., Stow, D., García, M., Somoza, L., Vazquez, J.T., Lobo, F., Maestro, A., Díaz del Rio, V., León, R., Medialdea, T., Gardner, J., 2006. The contourite depositional system of the Gulf of Cadiz: a sedimentary model related to the bottom current activity of the Mediterranean outflow water and its interaction with the continental margin. Deep-Sea Res. II Top. Stud. Oceanogr. 53 (11–13), 1420–1463. http://dx.doi.org/10.1016/ j.dsr2.2006.04.016.

Hernández-Molina, F.J., Llave, E., Stow, D.A.W., 2008. Continental slope contourites. In: Rebesco, M., Camerlengui, A. (Eds.), Contourites, Development in Sedimentology 60. Elsevier, Amsterdan, pp. 379–407.

Hernández-Molina, F.J., Stow, D.A.V., Alvarez-Zarikian, C., Expedition IODP 339 Scientists, 2013. IODP Expedition 339 in the Gulf of Cadiz and off West Iberia: decoding the environmental significance of the Mediterranean Outflow Water and its global influence. Sci. Drill. 16, 1–11. http://dx.doi.org/10.5194/sd-16-1.

Hernández-Molina, J., Stow, D.A.V., Alvarez-Zarikian, C.A., Acton, G., Bahr, A., Balestra, B., Ducassou, E., Flood, R., Flores, J.A., Furota, S., Grunert, P., Hodell, D., Jimenez-Espejo, F., Kim, J.K., Krissek, L., Kuroda, J., Li, B., Llave, E., Lofi, J., Lourens, L., Miller, M., Nanayama, F., Nishida, N., Richter, C., Roque, C., Pereira, H., Sanchez Goñi, M.F., Sierro, F.J., Singh, A.D., Sloss, C., Takashimizu, Y., Tzanova, A., Voelker, A., Williams, T., Xuan, C., 2014. Onset of Mediterranean outflow into the north Atlantic. Science 344, 1244–1250.

Hernández-Molina, F.J., Sierro, F.J., Llave, E., Roque, E., Stow, D.A.W., William, T., Lofi, J., Vand der Schee, M., Arnáiz, A., Ledesma, S., Rosales, C., Rodriquez-Tovar, F.J., Pardo-Igúzquiza, E., Brackenridge, R.E., 2016. Evolution of the Gulf of Cadiz and southwest Portuguese contourite depositional system: tectonic, sedimentary and paleoceanographic implication from IODP Expedition 339. Mar. Geol. 377, 7–39.

Hollister, C.D., Heezen, B.C., 1972. Geologic effects of ocean bottom current: western North Atlantic. In: Gordon, A.L. (Ed.), Studies in Physical Oceanography 2. Gorond and Breach, New York, pp. 37–66.

Hoogakker, B.A., Rothwell, R.G., Rohling, E.J., Paterne, M., Stow, D.A.V., Herrel, J.O., Clayton, T., 2004. Variation in terrigenous dilution in western Mediterranean Sea pelagic sediments in response to climate change during the last cycle. Mar. Geol. 211, 21–43.

Jenner, K.A., Piper, D.J.W., Campell, C., Mosher, D.C., 2007. Lithofacies and origin of late quaternary mass transport deposits in submarine canyons, central Scotia Slope, Canada. Sedimentology 54, 19–38.

Johnson, D., Rasmussen, K., 1984. Late Cenozoic turbidite and contourite deposition in the southern Brazil Basin. Mar. Geol. 58, 225–262.

Kenyon, N.H., Belderson, R.H., 1973. Bedforms of the Mediterranean undercurrent observed with side-scan sonar. Sediment. Geol. 9, 77–99.

Llave, E., Hernández-Molina, F.J., Somoza, L., Díaz del Río, V., Stow, D.A.V., Maestro, A., Alveirinho Dias, J.M., 2002. Seismic stacking pattern of the Faro–Albufeira contourite system (Gulf of Cádiz): a Quaternary record of paleoceanographic and tectonic influences. Mar. Geophys. Res. 22 (5–6), 487–508. http://dx.doi.org/10.1023/ A: 1016355801344.

Llave, E., Schönfeld, J., Hernádez-Molina, F.J., Mulder, T., Somoza, L., Díaz del Río, V., Sánchez-Almazo, I., 2006. High resolution stratigraphy of the Mediterranean outflow contourite system in the Gulf of Cadiz during the late Pleistocene: the impact of Heinrich events. Mar. Geol. 227, 241–262.

Llave, E., Hernández-Molina, F.J., Somoza, L., Stow, D.A.V., Díaz Del Río, V., 2007a. Quaternary evolution of the contourite depositional system in the Gulf of Cádiz. Geol. Soc. Lond., Spec. Publ. 276, 49–79. http://dx.doi.org/10.1144/GSL.SP.2007.276.01.03.

Llave, E., Hernández-Molina, F.J., Stow, D.A.V., Fernández-Puga, M.C., Garcia, M., Vázquez, J.T., Maestro, A., Somoza, L., Díaz del Río, V., 2007b. Reconstructions of the Mediterranean Outflow Water during the Quaternary base on the study of changes in buried mounded drift stacking pattern in the Gulf of Cadiz. Mar. Geophys. Res. 28, 379–394.

Lobo, F.J., Hernández-Molina, F.J., Somoza, L., Díaz del Río, V., 1999. Palaeoenvironments, relative sea-level changes and tectonic influence on the Quaternary seismic units of the Huelva continental shelf (Gulf of Cadiz, southwestern Iberian Peninsula). Bol. Inst. Esp. Oceanogr. 15, 161–180.

Lobo, F.J., Hernández-Molina, F.J., Somoza, L., Díaz del Rio, V., 2001. The sedimentary record of the post-glacial trangression on the Gulf of Cadiz shelf (Southwest Spain). Mar. Geol. 178, 171–195.

Lobo, F.J., Le Roy, P., Mendez, I., Sahabi, M., 2014. The Gulf of Cadiz Continental Shelves. In: Chiocci, F.L., Chivas, A.R. (Eds.), Continental Shelves of the World: Their Evolution During the Last Glacio-Eustatic Cycle. Geological Society, London Memoirs 41, pp. 109–130.

Locker, S.D., Laine, E., 1992. Paleogene-Neogene depositional history of the middle U.S. Atlantic continental rise: mixed turbidite and countourite depositional systems. Mar. Geol. 103, 137–164.

López-Galindo, A., Rodero, J., Maldonado, A., 1999. Surface facies and sediment dispersal pattern: south Gulf of Cádiz, Spanish continental margin. Mar. Geol. 155, 83–98.

Machado, A., Rocha, F., Gomes, C., Dias, J.A., Araújo, M.F., Gouveia, A., 2005. Mineralogical and geochemical characterization of surficial sediment from the south western Iberian continental shelf. Thalassas 21 (1), 67–76.

Maldonado, A., Stanley, D.J., 1976. Lithofacies as function of depth in the Strait of Sicily. Geology 5, 111–117.

Maldonado, A., Somoza, L., Pallarés, L., 1999. The Betic orogen and the Iberian-African boundary in the Gulf of Cadiz: geological evolution (central North Atlantic). Mar. Geol. 155, 9–43.

Maldonado, A., Rodero, J., Pallarés, L., Pérez, L., Somoza, L., Medialdea, T., Hernández-Molina, J., Lobo, F.J., 2003. Geological map of the Spanish Continental Shelf and adjacent areas. Scale 1:200.000. (ITGE-CSIC) Cadiz sheet, 86–86S–87S (Gulf of Cadiz). Spanish Geological Survey. Instituto Tecnológico Geominero de España, ITGE, Madrid (ISBN, 84-7840-478-3, 91 pp.).

Marchès, E., Mulder, T., Cremer, M., Bonnel, C., Hanquiez, V., Gonthier, E., Lecroart, P., 2007. Contourite drift construction influenced by capture of Mediterranean Outflow Water deep-sea current by the Portimão submarine canyon (Gulf of Cádiz, South Portugal). Mar. Geol. 242 (4), 247–260.

Marchès, E., Mulder, T., Gonthier, E., Cremer, M., Hanquiez, V., Garlan, T., Lecroart, P., 2010. Perched lobe formation in the Gulf of Cadiz: interactions between gravity processes and contour currents (Algarve Margin, Southern Portugal). Sediment. Geol. 229, 81–94.

Martínez-Ruíz, F., Comas, M.C., Alonso, B., 1999. Mineral association and geochemical indicators in the Upper Miocene to Pleistocene sediments in the Alboran Sea. In: Zhan, R., Comas, M.C., Klaus, A. (Eds.), Proceedings of the Ocean Drilling Program, Scientific Results 161, College Station, TX (Ocean Drilling Program), pp. 21–36.

McCave, I.N., Carter, L., 1997. Recent sedimentation beneath the deep western boundary current off northern New Zealand. Deep-Sea Res. 44 (7), 1203–1237.

McCave, I.N., Bryant, R.J., Cook, H.F., Coughanowr, C.A., 1986. Evaluation of a laser analyser for use with natural sediments. J. Sediment. Petrol. 56, 561–564.

Medialdea, T., Vegas, R., Somoza, L., Vázquez, J.T., Maldonado, A., Díaz del Río, V., Maestro, A., Córdoba, D., Fernández-Puga, M.C., 2004. Structure and evolution of the Olistostrome complex of Gibraltar Arc in the Gulf of Cadiz eastern Central Atlantic evidence from two long seismic section. Mar. Geol. 209, 173–198.

Mélières, F., 1974. Recherches sur la dynamique sédimentaire du Golfe de Cadix (Espagne) (Doctoral Thesis) University of Paris (nº A10206).

Mhammedi, A.N., El Moumni, B., El Hmaidi, A., Raissouni, A., El Arrim, A., 2008. Mineralogical and geochemical study of mud volcanoes in north Moroccan, Atlantic margin. African. J. Environ. Sci. Technol. 11, 387–396.

Miall, A.D., 1991. Stratigraphic sequences and their chronostratigraphic correlation. J. Sediment. Petrol. 61, 497–505.

Moral Cardona, J.P., Sánchez Bellón, A., López-Aguayo, F., Caballero, M.A., 1997. The analysis of quartz grain surface features as a complementary method for studying their provenance: the Guadalete River Basin (Cadiz, SW Spain). Sediment. Geol. 106, 155–164.

Moral Cardona, J.P., Gutiérrez Mas, J.M., Sánchez Bellón, A., Domínguez-Bella, S., Martínez López, J., 2005. Surface textures of heavy mineral grains: a new contribution to provenance studies. Sediment. Geol. 174, 223–235.

Morales, J.A., 1997. Evolution and facies architecture of the mesotidal Guadiana River delta (SE España–Portugal). Mar. Geol. 138, 127–148.

Mougenot, D., 1988. Géologie de la Marge Portugaise. Thèse 3éme Cycle. Univ. Pierre et Marie Curie, Paris, VI (259 pp.).

Mulder, T., Voisset, M., Lecroart, P., Le Drezen, E., Gonthier, E., Hanquiez, V., Faugères, J.-C., Habgood, E., Hernández-Molina, F.J., Estrada, F., Llave-Barranco, E., Poirier, D., Gorini, C., Fuchey, Y., Volker, A., Freitas, P., Lobo Sanchez, F., Fernandez, L.M., Morel, J., 2003. The Gulf of Cádiz: an unstable giant contouritic levee. Geo-Mar. Lett. 23 (1), 7–18.

Mulder, T., Lecroart, P., Hanquiez, V., Marches, E., Gonthier, E., Guedes, J.C., Thiébot, E., Jaidi, B., Kenyon, N., Voisset, M., Perez, C., Sayago, M., Fuchey, Y., Bujan, S., 2006. The western part of the Gulf of Cadiz: contour currents and turbidity current interactions. Geo-Mar. Lett. 26, 31–41.

Mulder, T., Faugères, J.C., Gonthier, E., 2008. Mixed turbidite–contourites systems. In: Rebesco, M., Camerlengui, A. (Eds.), Contourites, Development in Sedimentology. Elsevier, Amsterdan, pp. 435–456.

Mulder, T., Hassan, R., Ducassou, E., Zaragosi, S., Gonthier, E., Hanquiez, V., Marchès, E., Toucanne, S., 2013. Contourites in the Gulf of Cadiz: a cautionary note on potentially ambiguous indicators of bottom current velocity. Geo-Mar. Lett. 33, 357–367.

Nardin, T.R., Hein, F.K., Gorsline, D.S., Edwards, B.D., 1979. A review of mass movement processes, sediment and acoustic characteristics, and contrasts in slope and base-of-slope systems versus canyon-fan-basin systems. In: Dolye, L.J., Pilkey, O.H. (Eds.), Geology of Continental Slope. Society of Petroleum Economist Mineralogist, Spec. Publ. 27, pp. 61–73.

Nelson, C., Baraza, J., Maldonado, A., Rodero, J., Escutia, C., Barber, J.H., 1999. Influence of the Atlantic inflow and Mediterranean outflow currents on Late Quaternary sedimentary features of the Gulf of Cadiz continental margin. Mar. Geol. 155, 99–129.

Oliveira, J.T., Horn, M., Paproth, E.P., 1979. Preliminary note on the stratigraphy of Baixo Alentejo Flysch Group, Carboniferous of Portugal and on the paleogeographic development compared to corresponding units in the Northwest Germany. Cominicao Serv. Geol. Port. 65, 151–168.

Palanques, A., Díaz, J.I., Farrán, M., 1995. Contamination of heavy metals in the suspended and Surface of the Gulf of Cadiz (Spain): the role of sources, pathways and sink. Oceanol. Acta 18, 469–477.

Pearce, T.J., Jarvis, I., 1992. Composition and provenance of turbidite sands: Late Quaternary Madeira Abyssal Plain. Mar. Geol. 109, 21–51.

Perconig, E., Martínez-Díaz, P., 1977. Perspectivas petrolíferas de Andalucia Occidental. Bol. Geol. Min. 88, 417–433.

Piper, D.J.W., 1973. The sedimentology of silt turbidtes from the Gulf of Alaka. In: Kulm L.D., von Huene, R., et al. (Eds.). Initial Rep. Deep Sea Drill. Proj. 18, 847–867.

Ratzov, G., Collot, J.Y., Sosson, M., Migeon, S., 2010. Mass-transport deposits in the northern Ecuador subduction trench: result of frontal erosion over multiple cycles. Earth Planet. Sci. Lett. 296, 89–102.

Rea, D.K., Hovan, S., 1995. Grain size distribution and depositional processes of the mineral component of abyssal sediments: lesson from the North Pacific. Paleoceanography 10 (2), 251–258.

Rebesco, M., Stow., D.A.V., 2001. Seismic expression on contourites and related deposits: a preface. Mar. Geophys. Res. 22, 303–308.

Rebesco, M., Hernández-Molina, F.J., Van Rooij, D., Wahlin, A., 2014. Contourites and associated sediments controlled by deep-water circulation processes: state of the art and future considerations. Mar. Geol. 352, 111–154.

Rodríguez-Tovar, F.J., Dorador, J., 2015. Ichnofabric characterization in cores: a method of digital image treatment. Ann. Soc. Geol. Pol. 85, 465–471.

Rodríguez-Tovar, F.J., Dorador, J., Martín-García, G.M., Sierro, F.J., Flores, J.A., Hodell, D.A., 2015a. Response of macrobenthic and foraminifer communities to changes in deep-

sea environmental conditions from Marine Isotope Stage (MIS) 12 to 11 at the "Shackleton Site". Glob. Planet. Chang. 133, 176–187.
Rodríguez-Tovar, F.J., Dorador, J., Grunert, P., Hodell, D., 2015b. Deep-sea trace fossil and benthic foraminiferal assemblages across glacial Terminations 1, 2 and 4 at the "Shackleton Site" (IODP Expedition 339, Site U1385). Glob. Planet. Chang. http://dx.doi.org/10.1016/j.gloplacha.2015.05.003.
Roldán-García, E.J., García-Cortés, A., 1988. Implicaciones de los materiales triásicos en la Depresión del Guadalquivir (provincias de Córdoba y Jaén). Proceedings II Congreso Geologico de España, I, pp. 189–192.
Roque, C., Hernández-Molina, F.J., Lobo, F., Somoza, L., Días del Río, V., Vázquez, J.T., Dias, J., 2010. Geomorphology of the Eastern Algarve proximal continental margin (South Portugal, SW Iberian Peninsula): sedimentary dynamic and its relationship with the last asymmetrical eustatic cycle. Cienc. Tierra 17, 7–28.
Roque, C., Duarte, H., Terrinha, P., Valadares, V., Noiva, J., Cachao, C., Ferreira, J., Legoinha, P., Zitellini, N., 2012. Pliocene and Quaternary depositional model of the Algarve margin contourites drifts (Gulf of Cadiz, SW Iberia): seismic architecture, tectonic control and paleoceanographic insights. Mar. Geol. 303-306, 42–62.
Rosa, F., Rufino, M.M., Ferreira, O., Matias, A., Brito, A.C., Gaspar, M.G., 2013. The influence of coastal processes on inner shelf sediment distribution: the eastern Algarve shelf (Southern Portugal). Geol. Acta 11 (1), 59–73.
Shanmugam, G., 1997. The Bouma Sequence and the turbidte mind set. Earth-Sci. Rev. 42, 201–229.
Shor, A.N., Kent, D.V., Flood, R.D., 1984. Contourite or turbidite?: magnetic fabric of fine Quaternary sediments, Nova Scotia continental rise. Geol. Soc. Lond. 15, 257–273.
Siesser, W.G., Rogers, J., 1976. Authigenic pyrite and gypsum in south-east African continental slope sediments. Sedimentology 23, 567–577.
Stanley, D.J., 1987. Turbidite to current-reworked sand continuum in upper Cretaceous rocks, US. Virgin Islands. Mar. Geol. 78, 143–151.
Stanley, D.J., 1993. Model for turbidite-to-continuum and multiple process transport in deep marine settings: examples in the rock record. Sediment. Geol. 82, 241–255.
Stow, D.A.V., 1979. Distinguishing between fine-grained turbidites and contourites on the Nova Scotian deep water margin. Reprint. Sedimentol. 26, 371–387.
Stow, D.A.V., Faugères, J.C., 2008. Contourites facies and the facies model. In: Rebesco, M., Camerlengui, A. (Eds.), Contourites, Development in Sedimentology. Elsevier, Amsterdam, pp. 223–256.
Stow, D.A.V., Shanmugam, G., 1980. Sequence of structure in fine-grained turbidites: comparison of recent deep-sea and ancient flysch sediments. Sediment. Geol. 25, 23–42.
Stow, D.A.V., Faugères, J.C., Gonthier, E., 1986. Facies distribution and textural variation in Faro Drift contourites: velocity fluctuation and drift growth. Mar. Geol. 72, 151–166.
Stow, D.A.V., Faugères, J.C., Gonthier, E., Cremer, M., Llave, E., Hernández-Molina, F.J., Somoza, L., Díaz del Río, V., 2002. Faro-Albufeira Drift Complex, Northern Gulf of Cádiz. In: Stow, D.A.V., Pudsey, C.J., Howe, J.A., Faugères, J.-C., Viana, A.R. (Eds.), Deep-Water Contourite Systems: Modern Drifts and Ancient Series, Seismic and Sedimentary Characteristics. Geol. Soc. Lond. Mem. 22(1), pp. 137–154.
Stow, D.A.V., Hernández-Molina, F.J., Alvarez Zarikian, C.A., the Expedition 339 Scientists, 2013. Proceedings IODP, 339. Integrated Ocean Drilling Program Management International, Tokyo. http://dx.doi.org/10.2204/iodp.proc.339.
Takashimizu, Y., Kawamura, R., Rodríguez-Tovar, F.J., Dorador, J., Ducassou, E., Hernández-Molina, F.J., Stow, D.A.V., Alvarez-Zarikian, C.A., 2016. Reworked tsunami deposits by bottom currents: circumstantial evidences from Late Pleistocene to Early Holocene in the Gulf of Cádiz. Mar. Geol. 377, 95–109.
Talling, P.J., Amy, L.A., Wynn, R.B., Peakal, J., Robinson, M., 2004. Beds comprising debrite sandwiched within co-genetic turbidite: origin and widespread occurrence in distal depositional environments. Sedimentology 51, 163–194.
Toucanne, S., Mulder, T., Schönfeld, J., Hanquiez, V., Gonthier, E., Duprat, J., Cremer, M., Zaragossi, S., 2007. Contourites of the Gulf of Cadiz: a high-resolution record of the paleocirculation of the Mediterranean outflow water during the last 50,000 years. Palaeogeogr. Palaeoclimatol. Palaeoecol. 246, 354–366.
Tripsanas, E.K., Piper, D.J.W., Jenner, K.A., Bryan, W.R., 2008. Submarine mass-transport facies: new perspectives on flow processes from cores on the eastern North American margin. Sedimentology 55, 97–136.
Vergnaud-Grazzini, C., Caralp, M., Faugères, J.C., Gonthier, E., Grousset, F., Pujol, C., Saliège, J.F., 1989. Mediterranean outflow through the Strait of Gibraltar since 18,000 year BP. Oceanol. Acta 12 (4), 305–324.
Viana, A.R., 2001. Seismic expression of shallow-to deep-water contourites along the south. Eastern Brazilian margin. Mar. Geophys. Res. 22, 509–521.
Viana, A.R., Faugères, J.C., Kowsmann, R.O., Lima, J.A.M., Caddah, L.F.G., Rizzo, J.G., 1998. Hidrology, morphology and sedimentology of the Campos Continental margin. Offhshore Brazil. Sediment. Geol. 115 (1–4), 133–158.
Vidal, J.R., Cáceres, L.M., Ramírez, A.R., 1993. Modelo evolutivo da rede fluvial Cuaternaria en el suroeste de la península Ibérica. Actas 3ª Reuniao do Quaternario Ibérico. Universidad de Coimbra, pp. 93–96.
Walker, R.G., 1965. The origin and significance of the internal sedimentary structures of turbidites. Proc. Yorks. Geol. Soc. 35, 1–32.
Weaver, P.P.E., Rothwell, R.C., 1987. Sedimentation on the Madeira Abyssal Plain over the last 300,000 years. In: Weaver, P.P.E., Thomson, J. (Eds.), Geology and Geochemistry of Abyssal Plains. Geol. Soc. London, Sp. Publ. 31, pp. 71–86.
Weller, J.M., 1958. Stratigraphic facies differentiation and nomenclature. Facies and the Reconstruction of Environments. Bulletin of the American Association of Petroleum Geologist 42 (3), pp. 609–639.
Wetzel, A., 2007. Bioturbation in Deep-sea Fine Grained Sediments: Influence of Sediment Texture, Turbidite Frequency and Rates of Environmental Change. Geological Society London, Sp. Publ. 15 pp. 595–608.
Wynn, R.B., Weaver, P.P.E., Masson, D.G., Stow, D.A.V., 2012. Turbidite depositional architecture across three interconnected deep-water basins on the north-west African margin. Sedimentology 49, 669–695.
Zaho, Y., Liu, Z., Colin, C., Xie, X., Wu, Q., 2011. Turbidite deposition in the southern South China Sea during the last glacial: evidence form grain-size and major elements records. Chin. Sci. Bull. 56 (33), 3558–3565.
Zitellini, N., Gracia, E., Matias, L., Terrinha, P., Abreu, M.A., DeAlteriis, G., Henriet, J.P., Dañobeitia, J.J., Masson, D.G., Mulder, T., Ramella, R., Somoza, L., Diaz, S., 2009. The quest for the Africa-Eurasia plate boundary west of the Strait of Gibraltar. Earth Planet. Sci. Lett. 280, 13–50.